DATA ANALYSIS OF PERMANENT GPS NETWORKS IN ITALY AND SURROUNDING REGIONS: APPLICATION OF A DISTRIBUTED PROCESSING APPROACH

E. SERPELLONI*[1], G. CASULA[1], A. GALVANI[2], M., ANZIDEI[2] and P. BALDI[3]

[1] Istituto Nazionale di Geofisica e Vulcanologia, Centro Nazionale Terremoti - Sede di Bologna; V. Donato Creti, 12, 40128 Bologna, Italy. * Corresponding author: phone: +39 051 4151433, Fax: +39 051 4151489, E.mail: serpelloni@bo.ingv.it

[2] Istituto Nazionale di Geofisica e Vulcanologia , Centro Nazionale Terremoti; Via di Vigna Murata, 605, Roma 00143, Italy

[3] Dipartimento di Fisica, Università di Bologna; V.le C.B. Pichat, 8, 40127 Bologna, Italy.

Abstract We describe the procedures used to combine into a uniform velocity solution the observations of more than 80 continuous GPS stations operating in the central Mediterranean in the 1998-2004 time interval. We used a distributed processing approach, which makes efficient use of computer resources, while producing velocity estimates for all stations in one common reference frame, allowing for an effective merging of all the observations into a self-consistent network solution. We describe the CGPS data archiving and processing procedures, and provide main results in terms of position time-series and velocities for all stations that observed more than three years. We computed horizontal and vertical velocities accounting for the seasonal (annual and semi-annual) signals, and considering the off-sets in the coordinate time-series caused by station equipment changes. Weighted post-fit RMS of the north, east and vertical velocity components are in the range of 1.57-2.08 mm, 1.31-3.28 mm, and 3.60-7.24 mm, respectively, which are reduced by solving for seasonal signals in the velocity estimates. The annual and semi-annual signals in the height components, with amplitudes up to 4.8 mm, are much stronger than those in the horizontal components. The mean amplitudes of annual and semi-annual signals are within 0.18-0.47 mm, 0.23-0.52 mm and 0.55-1.92 mm in the north, east and vertical components, respectively.

Key words: Global Positioning System (GPS), Continuous Monitoring, Central Mediterranean, Time Series Analysis.

1. INTRODUCTION

The rapid development of modern space geodesy techniques over the last two decades provided new important data that introduced significant constraints on the active geological processes occurring in the Mediterranean area (e.g., Battaglia *et al.*, 2004; D'Agostino and Selvaggi, 2004; Goes *et al.*, 2004; D'Agostino *et al.*, 2005; Serpelloni *et al.*, 2005 among others). Earlier GPS studies used either very large or sparse global networks (e.g., Larson *et al.*, 1997), focusing only on the large scale tectonics aspects (i.e., the motion of major tectonic plates, intra-plate rigidity), or dense but small aperture networks, focusing only on local tectonic processes, such as deformation along particular segments of fault zones (e.g., Anzidei *et al.*, 1998). The difficulties to tie such a different scale networks into a common reference frame has been one of the main obstacles in understanding the active tectonic processes in diffusely deforming continental plate boundaries, which are of great scientific interest for seismic hazard aspects. During the last 10 years, the rapid development of the global GPS technique, mainly under the umbrella of the International GPS Service for Geodynamics consortium (IGS; http://igscb.jpl.nasa.gov), provided more precise determination of satellite orbital parameters, through the enlargement of the GPS satellite constellation, and the improvement of the global Continuous GPS (CGPS) tracking station coverage. Moreover, the establishment of regional networks of CGPS stations (e.g., EPN-EUREF, ASI, Regal, FredNet networks) increased the number of stations available to tie observations together interferometrically. This technological development significantly increased the precision of station position determinations, reducing the noise spectra of the solutions, and allowing for a better resolution of the coordinate changes detection, even in the vertical component. This is fundamental in areas characterized by low deformation rates, such as the western and central Mediterranean and the European region (McClusky *et al*., 2003; Nocquet and Calais 2003), where an accurate estimate of crustal deformation parameters require mainly the use of CGPS stations.

In Italy, several CGPS stations are operated and managed by different agencies, private companies and national scientific institutions (see Sansò and De Lacy, available at http://geomatica.como.polimi.it/gps/articoli/asi.pdf), but have been built for different purposes (i.e., topography, cartography, telecommunication, crustal deformation monitoring, navigation, etc…). Unfortunately, the number of sites that match the

minimum requirements needed for geophysical applications (antenna/receiver features and monumentation quality), and for which raw data are freely available on the internet is actually not enough to provide an exhaustive description of the deformation pattern of such a high tectonically fragmented zone. For this reason, at present days, the use of high quality non-permanent GPS data, collected over significantly long time span (at least 5 years) by means of repeated campaigns, is still fundamental to improve the spatial and temporal resolution of the crustal deformation field in the study area (e.g., Serpelloni *et al*., 2002, 2005).

In the last years the number of CGPS stations suitable for geophysical applications is rapidly increasing, particularly in the frame of INGV activities. In this prospective, we developed automatic facilities to handle the CGPS data archiving and data processing procedures. In this work we present an application of the "distributed processing" technique, used to merge most of the available CGPS networks operating in the central Mediterranean, with the goal of obtaining a single network solution, and formally no more considering the different networks separately. The data analysis approach followed allows us to obtain velocity vectors of stations belonging to networks whose raw data are not directly processed. We describe in details the procedures used to collect, archive and process the raw data in order to combine all these information into one uniform crustal velocity field. Results can be further used for geo-kinematics purposes, and for a better understanding of the active geodynamic processes that are deforming the Earth's surface in Italy and surrounding regions. A detailed tectonics interpretation of the presented results is, however, out of the scope of this work.

2. CONTINUOUS GPS NETWORKS IN THE STUDY AREA

In the last ten years the number of CGPS sites operating in the central Mediterranean region significantly increased. Since the number of stations belonging to the global and European networks (i.e., IGS and EUREF networks) is still too small, in order to enlarge our analysis outside Italy we collect and process data coming from other regional CGPS networks in France and Austria. Figures 1a and 1b show the distribution of the 81 CGPS stations for which we routinely download and process raw data to produce position time-series. Table 1 reports some information related to these sites, which belong to the networks described in the following paragraphs.

IGS. The International GPS Service, along with a multinational membership of organizations and agencies, maintains a global network of over 350 continuously operating dual-frequency GPS stations, which provides high-quality data on line in near real time. These data sets are used by the IGS to generate several data products (i.e., GPS satellite ephemeredes, Earth rotation parameters, tracking station coordinates and velocities, GPS satellite and IGS tracking station clock information, Zenith tropospheric path delay estimates, global ionospheric maps, etc …), available through the Internet. The accuracies of IGS products are sufficient for the improvement and extension of the International Terrestrial Reference Frame (ITRF), the monitoring of solid Earth deformations, the monitoring of Earth rotation and variations in the fluid Earth (sea level, ice-sheets, etc.), for high precision satellite orbit determinations, ionosphere and troposphere studies. While from a constructive point of view the IGS network is largely heterogeneous, the stations have to meet some restricted requirements, both in terms of data quality and monument stability trough time. We currently download and analyze the raw data coming from 11 IGS stations in the Euro-Mediterranean region (black squares in Fig.1a and 1b; NYA1 is outside map), which have been chosen to constitute the sub-set of sites that are in common to all the sub-networks analyzed and allows for further combinations.

EUREF. The EUREF Permanent Network (EPN; http://epncb.oma.be/) represents the densification of the IGS network in Europe, and has been setup starting from 1995. The EPN is a science-driven network of permanent GPS tracking stations whose weekly computed positions are used by EUREF to realize the European Terrestrial Reference System. The EPN is also valuable for scientific applications, such as geodynamics, sea level monitoring and weather prediction. More than 150 EPN stations, distributed over 32 European countries, provide near real time high quality GPS data, archived at local and regional data centers. EPN analysis centers routinely analyze the data from this network and deliver to the GPS community data products, including precise coordinates for all stations, satellite ephemeredes, Earth orientation parameters (EOP), etc. The EPN tracking stations are integrated in the successive realizations of the International Terrestrial Reference System. As for the IGS network, also the EPN stations must follow some restricted requirements in terms of data quality and monument stability. However, the large part of these stations are built on roof of buildings or set up with quite poor monuments, which can reduce the tectonic

significance of the detected signal. We routinely process the data coming from 25 EPN stations, which are located in and around the Italian region (see Fig.1a and 1b).

ASI. The Italian Space Agency (ASI), since 1995, established some permanent GPS stations to constitute the Italian GPS Fiducial Network, together with some of the fundamental stations, like Matera (belonging to the IGS core sites network), active from the 1991. The ASI network (http://geodaf.mt.asi.it/html/browse.html) is constituted by 32 stations, some of them belonging to other networks (e.g., IGS, EPN, INGV and Frednet). This network includes stations for which data and monument quality requirements are not as tight as for the IGS and EPN networks. ASI stations, in fact, display a large variability of monument typologies and antenna/receiver combinations, and most of them are built on roof of buildings. Standard station log-files are available on the GEODAF web site. We analyze all the RINEX data coming from the ASI network.

INGV. The Istituto Nazionale di Geofisica e Vulcanologia (INGV), since 1997 began to setup a permanent GPS network in Italy. The network has been established with the aim to detect crustal deformation for geodynamics, seismic hazard and civil protection goals. The network considered in this work is constituted by 6 stations (Fig. 1b). The number of vertices is rapidly increasing over the Italian region, either in correspondence of the new and old INGV seismic stations or independently from them. The GPS monuments are realized by means of reinforced concrete pillars, linked to the coherent rock outcrops or deeply anchored in non consolidated deposits. The GPS antenna is connected to the pillar by means of two different devices: the INGV-3D antenna mount (http://www.ingv.it/labtel2/ufpage.htm) and the SCIGN antenna mount (http://jacinto.ucsd.edu/gpsmon/adaptor_design/intro.html). For some of the stations the raw data are daily transferred on a server, for other, where telemetric connection is still not available, the raw data are downloaded locally and later archived.

FREDNET. The Friuli Regional Deformation Network (FREDNET; http://www.crs.inogs.it/frednet/) is operated and maintained by the Centro Ricerche Sismologiche (CRS) of the Istituto Nazionale di Oceanografia e di Geofisica Sperimentale, in Udine. The network has been installed to monitor crustal deformation along the northeastern boundary of the Adriatic microplate. The goal is to estimate interseismic strain accumulation on active faults for a better assessment of the regional seismic hazards, but also to provide infrastructure for geodetic data management and

processing. The network is presently constituted by 8 stations, characterized by high and uniform construction standards. Most of the stations are built on stable rock outcrops (with the exception of UDIN and TRIE, which are located on buildings) and all are equipped with the same GPS equipment. The choke-ring antennas, covered with a SCIGN dome, are mounted on a 1-m reinforced concrete pillar founded in the surface bedrock by means of epoxied metal rods. Since most of the stations are located on remote areas, cellular modems are used to telemeter the data to the local archive. All the data of this network are routinely analyzed.

REGAL. The Réseau GPS permanent dans les Alpes network (REGAL; http://kreiz.unice.fr/regal/) is a permanent GPS array located in the western Alps and their surroundings. The network, which is dedicated to crustal deformation monitoring (Calais *et al*., 2000), started operating in 1997 and currently consists of 22 stations, some of which contributes to the France RGP (Reseau GPS Permanent) and EUREF networks. The REGAL station monuments are mainly concrete pillars founded on stable bedrock, equipped with choke-ring antennas. We analyze data from 7 stations, selected considering their data availability trough time and their monumentation quality.

AUSTRIA. The Austrian Continuous GPS Network is constituted by more than 35 stations, some of them contributing to the EUREF network, and is operated by the Department of Satellite Geodesy of the Austrian Accademy of Science (http://www.iwf.oeaw.ac.at/english/research/earth/geodynamics/gps_e.html). This network has been established to investigate geodynamic processes in the eastern alpine region, but also for commercial applications, such as mapping and cadastral purposes. We do not process observations from the whole network, but we analyze data from 5 sites selected using as criteria the data availability trough time and the monument quality (when available as information on the web site).

OTHER. Other CGPS stations are presently operating in the Italian region. Some of them have been installed in the frame of national projects (i.e., CADM), some other are maintained by University departments (ASIA, BASO, BRAS and ROVI), or by Administrative agencies (MERA and TREN).

3. RINEX DATA ARCHIVING

In order to manage the large amount of data coming from the CGPS networks considered, we developed several procedures, under Linux operating system, to setup an

archive for RINEX data and meta-data (i.e., orbits) files. We used the File Transfer Protocol (FTP), automated by means of Bourne Shell (BASH) and Enhanced Courne Shell (CSH, TCSH) scripts and FORTAN77 programs, to download and archive RINEX files from remote ftp archives and to check antenna/receiver inconsistencies. This is crucial to maintain a database of observations that follows the IGS standards, and to built an historical record of stations equipment changes.

Figure 2 displays a flow-chart of the data archiving steps. On a weekly basis, we download RINEX data from several remote FTP archives (listed in Table 1), and archive them, together with orbits (precise and broadcast) and station information (i.e., station log-files). Considering that some of the sites collected display inconsistencies and errors in their RINEX file headers (e.g., wrong antenna/receiver codes and/or wrong antenna heights), which can significantly affect the data processing or further interpretations, an important module of the archiving procedures is devoted to the detection and correction of such errors to IGS standards (ftp://igscb.jpl.nasa.gov/igscb/data/format/rinex210.txt). To perform this task we developed several automated programs, both using FORTAN77 and BASH, which make use of the Unavco-TEQC software for GPS data and meta-data handling (http://www.unavco.org/facility/software/teqc/teqc.html).

Station information required to process and interpret GPS observations are obtained for most of the stations from the *station.info* table (ftp://lox.ucsd.edu/gamit/table), a machine readable file that lists the equipment history (i.e., receiver, antenna, offsets, agencies, domes, firmware, and the epochs of any change in the station configuration) of all the CGPS stations archived and processed by the Scripps Orbit and Permanent Array Center (SOPAC; http://sopac.ucsd.edu) of the University of California in San Diego. This file is derived by a daily analysis, through the SOPAC's Oracle Relation Database Management System (RDBMS), of all the standard log-files archived at SOPAC. For other sites not included into the SOPAC data base, these information are retrieved from EUREF-EPN historical station equipment configuration summary file (available at http://www.epncb.oma.be/ftp/station/general/extlog.hst) or directly from the station-log-files.

It is worth noting that some of the CGPS stations considered in this work (labeled as LOCAL in Table 1) are presently collecting data locally, and do not transmit

data to remote archives. For this reason their RINEX files are checked and archived only when available. For some other stations the RINEX data are not freely available on the Internet, and we process these data in agreement with the local operating institutions (labeled as CONV in Table 1).

At the end of the archiving procedure, the standard RINEX files are compressed, using the Hatanaka format (http://igscb.jpl.nasa.gov/mail/igsmail/1998/msg00012.html), and stored in the archive, which is maintained on a weekly basis. Ancillary data required to analyze the GPS phase observations, including broadcast ephemeredes and apriori orbits, stations coordinates and velocities, Earth orientation parameters, UT1 and Leap Second tables, are weekly retrieved from CDDIS (ftp://cddisa.gsfc.nasa.gov/) and SOPAC archives. All files are collected weekly, just prior to subsequent processing, and stored in the orbits and tables archives (see Fig. 2). We use the final SOPAC orbits (in g-file format, the internal GAMIT format), instead of the final IGS orbits, in order to maintain the highest homogeneity and uniformity in combining our solutions with the SOPAC regional and global ones.

4. CGPS DATA PROCESSING

Determining a self consistent set of station velocities from a vast amount of space geodetic data requires methods for reducing the large number of raw GPS observations to geodetic parameter estimates, such as site positions and velocities, Earth orientation parameters, satellite orbital parameters, and methods for combining the results to form a set of velocities in a uniform reference frame. The technique of CGPS is severely affected by problems of data volume and data consistency and, computationally, it is not feasible to treat all of the data available from the hundreds of stations operating in the Mediterranean and European region on any given day simultaneously. Over the last several years, however, some techniques have been developed to make efficient use of the ever growing GPS data set using the computational resources available (Blewitt *et al*., 1993). These techniques, which are defined as "distributed processing" approach, also provide a convenient means of combining results from different space geodetic techniques (i.e., Dong *et al*., 1998), such as VLBI, SLR, and campaign GPS measurements, while preserving uniformity in the reference frame definition. The basic approach is to analyze the data in subnetworks (clusters of stations), and then combine the subnetwork solutions using procedures

analogous to sequential least squares (i.e., Kalman filter). Because subnetworks are processed separately, this strategy affords also for the opportunity to combine the reduced data products derived from different techniques and by different analysts at different institutions, saving a very large amount of time and effort. The SOPAC facility routinely analyzes, starting from 1991, RINEX data coming from several CGPS networks all over the world, including the entire IGS network, and a sub-set of EUREF-EPN stations. The SOPAC facility provides to the scientific community daily loosely constrained solutions for all the networks they archive, and we took advantage of the distributed processing mode by not processing stations already analyzed by SOPAC, but choosing a set of IGS and EUREF stations that are in common between our three regional subnetworks and SOPAC global/regional ones (stations reported in Fig. 1a and 1b with black squares, plus NYA1 that is outside the map).

Another important feature of the distributed processing approach is that the reference frame is not defined until the last step of the analysis. This is achieved by applying loose constraints to all parameters (site positions, satellite orbital parameters, Earth orientation parameters) when reducing the raw data such that reference frame indeterminacy is regularized, but without affecting the invariant properties of the parameters estimates (i.e., Herring *et al*., 1991; Heflin *et al*., 1992). Moreover, this approach, based on the "quasi-observation" theory (Dong *et al*., 1998), allows for a rigorous combination of CGPS and non-permanent networks. Hence, different analysts can share data products without having to worry about the particular values the other analysts adopted to define their reference frames. Although we do not "fix" orbital and Earth orientation parameter estimates to precise values, we do use precise values for these parameters provided by the SOPAC facility as it benefits data editing and analyses.

The RINEX data coming from more than 80 stations (Table 1) are routinely processed using the GAMIT/GLOBK software (King and Bock, 2000), installed on two Linux machines, equipped with Intel-Pentium 4 processors and 1 GB of RAM memory, and a SUN-Ultrasparc station. Considering that the stations analyzed are equipped with largely different GPS instruments (i.e., different receivers and antennas), building clusters using the GPS equipment as criteria, which would be the best solution in order to avoid antenna mixing, is not practically feasible with the computational facilities available. For this reason we first used a geographical criteria, dividing the network into

two main subnetworks, a northern and a southern one. We than set-up a third cluster for all the stations that display lower regularity in the data availability, or that, in previous analysis, displayed lower data quality. In Table 1 the belongings of each station to the three clusters is also given.

Our raw data analysis procedure is divided into three main steps that include the phase data analysis, the combination of solutions and the position time-series analysis (Fig. 3). Each step is performed by means of three different software packages. The same processing scheme is applied uniformly to each day of the 5 years analysis considered in this work, but considering that changes in weighting schemes and software versions are thought to have minimal effects on the coordinate time-series. At the end of the three steps we obtain three dimensional motion rates in the most recent release of the ITRF frame.

4.1 Raw Data Reduction

The first step is performed through the GAMIT module, which uses double-differenced, ionosphere-free linear combinations of the L1 and L2 phase observations to generate weighted least square solutions for each daily session (King *et al*., 1985; Bock *et al*., 1986; Schaffrin and Bock, 1988; Dong and Bock, 1989). An automatic cleaning algorithm (AUTOCLN; for more details see Herring, 2000, King and Bock, 2000) is applied to postfit residuals, in order to repair cycle slips and to remove outliers; no attempt is usually made to recover edited data using manual techniques. The observation weights vary with elevation angle and are successively derived individually for each site from the scatter of postfit residuals obtained in a preliminary solution. Estimated parameters for each daily solution include the 3-dimensional Cartesian coordinates for each site, 6 orbital elements for each satellite (semi-major axis, eccentricity, inclination, longitude of ascending node, argument of perigee, and mean anomaly), Earth orientation parameters (pole position and rate and UT1 rate), and integer phase ambiguities (more details about bias-fixing procedures can be found in Serpelloni *et al*., 2002). We also estimate hourly piecewise-linear atmospheric zenith delays at each station to correct the poorly modeled troposphere, and 3 east-west and north-south atmospheric gradients per day, to account for azimuthal asymmetry; the associated error covariance matrix is also computed and saved. The elevation cutoff is set to 10° and we use the IGS elevation dependent models for modeling the effective

phase center of the receiver antennas. The effect of solid-earth tides, polar motion and oceanic loading are taken into account. Diurnal, semidiurnal and long period tide components are modeled according to the IERS/IGS standard 1996 (IERS Tech. Notes, 21, 1996). The correction for the polar motion are computed following the IERS convention (McCarthy, 1996); the largest period modeled is the Chandler Wobble (about 460 days). The oceanic loading correction is based on the Scherneck model (Scherneck, 1991), where amplitudes and phase of 11 components are determined.

The three subnetworks (see Tab. 1) are processed in parallel, with 11 overlapping "tie" sites included in each cluster, to provide a means of combining the individual solutions later in GLOBK, and also with the solutions given by SOPAC.

The basic products of this step are loosely-constrained solutions for each subnetwork, containing set of one-day site position estimates, Earth orientation parameters, and associated error covariance matrices. For the second step of the analysis it is also convenient to save in addition the satellite orbital parameter estimates. These data products, together with the loosely-constrained "*h*-file" solutions provided by SOPAC for the IGS1, IGS2, IGS3, IGS4, IGS5, EURA and EMED subnetworks (more information can be found at the SOPAC web page: http://sopac.ucsd.edu/processing/gamit/), are stored in the ASCII "*h*-file" format to form the *h*-file archive (see Fig. 3). In the following discussion we refer to the vector of parameter estimates derived from the raw data from the *k*th subnetwork as h_k, with H_k denoting the associated variance-covariance matrices.

4.2 Combination of Loosely Constrained Solutions

Once the loosely-constrained GPS parameter estimates from the individual GAMIT solutions (h_k, H_k) are obtained from the analysis of each subnetwork, these are combined using the GLOBK software (Herring, 2000) to form a daily unconstrained combined network solution (h_T, H_T). As in all intermediate steps, in our procedures the reference frame is only loosely defined in forming these combined network solutions. We effectively achieve this by solving the system of equations

$$\begin{aligned} h_1 &= A_1 h_T + e_1 \\ h_2 &= A_2 h_T + e_2 \\ &\vdots \\ h_k &= A_k h_T + e_k \end{aligned}$$

where k is the total number of subnetworks being combined (in this case 10), A_k are design matrices which related the total parameter set h_T to the kth subset h_k, and e_k represent the errors in the estimates h_k such that $Ee_k e_k^T = H_k$, where E is the mathematical expectation operator. The h_T vector contains estimates for the site positions and Earth orientation parameters at the epoch T. We compute one total network solution for each day, which is stored in the binary GLX format (binary GLOBK format for the loosely-constrained bias-fixed solutions) and archived (see Fig. 3). These files are thus converted into ASCII QOB (Quasi-Observation) file format, and stored in the QOB archive (see Fig. 3). It is worth noting that after combination into total network solution, we no longer need and retain the satellite orbital parameter estimates. A more detailed description of the mathematics involved in data combination and specific implementation in the GLOBK software can be found in Herring *et al*. (1990), Dong *et al*. (1998), and Herring (2000).

One of the main advantages of the adopted processing scheme is that the obtained QOB files carry the position time-series of all the CGPS stations included into the subnetworks we combined, that is more than 320 sites, distributed all over the Earth's surface. This allows for further tectonic studies at different scales, from the local fault segment scale to the global plate motion scale, using a uniform and self-consistent set of three dimensional station velocities. Figure 4a and 4b display the sites for which we have position time-series available.

4.3 Position Time Series Analysis and Velocity Estimate

The loosely constrained daily combined solutions (in ASCII QOB format) are input as quasi-observations to the Quasi-Observation Combination Analysis (QOCA) software (available at http://gipsy.jpl.nasa.gov/qoca), which is used to define a common reference frame, deriving the position time-series for all the stations. For each daily QOB file the network constraint solution (see Dong *et al*., 1998, Appendix C) is constructed using the 50 globally distributed core sites listed in Table 2. A seven-parameter transformation (three network rotations, three network translations, and one scaling parameter) is performed, aligning each solution to the 2000 realization of the International Terrestrial Reference Frame (Altamini, 2002).

The particular set of stations used to define the global reference frame is chosen in order to provide optimal global stability over time, but not only over the time interval

considered in this work. In fact, since the current network of IGS core sites was not complete until 1997 and one of our goal is also to combine continuous and non permanent GPS observations from the early nineties (Serpelloni *et al*., 2002) as uniformly as possible, the IGS core sites are supplemented with other stations (Table 2) characterized by a very long history and good-quality data, and with positions and velocities well-determined in the ITRF2000, or at least in the ITRF97. For the selected core stations we assume rates equal to the current site rates estimated in the ITRF2000 solution (Altamini *et al*., 2002). Since the vertical coordinates usually have poorer accuracy than the horizontal ones, we reduced the weight of vertical positions at core sites by a factor 100, in determining the 7 network parameters.

The observed motion $f(t)$ of each site in each direction (north, east, up) can be written as (e.g., Ding *et al.*, 2005):

$$f(t_i) = a + bt_i + c\sin(2\pi t_i) + d\cos(2\pi t_i) + e\sin(4\pi t_i) + f\cos(4\pi t_i) + \sum_{j=1}^{n_g} g_j H(t_i - T_{gj}) + \varepsilon_i$$

where t_i for $i = 1 \ldots N$ are the daily solutions epochs in units of years, and H is the Heaviside step function (Abramowitz and Stegun, 1972). The first two terms are the constant bias with respect to 1998.00, a, and the linear rate, b, respectively. Coefficients c and d describe the annual periodic motion, while e and f describe the semi-annual motion. The next term corrects for any number (n_g) of offsets, with magnitudes g and epochs T_g. In some time-series, in fact, there are offsets due mainly to antenna or receiver changes, which we model as step functions. Assuming that the offset epochs are known, the model is linear with respect to the coefficients. How epochs of equipment changes are derived is described in this work in the data archiving section.

Because of the existence of abnormal outliers in daily solutions, so that the scatter does not obey Gaussian statistics, the robust-fit algorithm embedded in the QOCA software, which resists outliers better than conventional least squares (Bock *et al*., 2000), is employed to estimate all the parameters simultaneously.

Table 3 provides the time-series parameters described above and derived for the central Mediterranean stations that observed for more than 3 years, and in particular the annual and semiannual amplitudes (c, d, e and f) terms, referred to January 1*th*, the Weighted Root Mean Squares (WRMS) of the time-series after removal of constant slope (velocity), and the computed offsets values, with 1σ uncertainties, are listed. ITRF2000 horizontal and vertical velocities, with 1σ uncertainties, are listed in Tab. 4.

The north, east and up detrended position time-series, with annual and semi-annual signals, for the Italian stations are shown in Figures 5a, 5b, 5c and 5d.

4.4 GPS Rate Error Estimate

The use of least-squares procedures to compute station velocities from position time-series provides formal uncertainties that are rather unrealistic. The usual assumption that measurement errors are random and uncorrelated from one epoch to the next (white noise), in fact, is violated with GPS data (Johnson and Agnew, 1995). The source of time-correlated (colored) noise in GPS data includes orbits, atmospheric effects and monument motions (Langbein and Johnson, 1997; Mao *et al*., 1999). If colored noise is present, but only pure white noise is assumed, GPS velocity errors can be significantly underestimated (Zhang *et al*., 1997). Williams *et al*., (2004) studied the position time-series of 414 CGPS sites, and confirmed previous studies, suggesting that white and flicker noise are clearly the dominant noise model, although there are more sites in their solutions where white noise plus random walk noise is the preferred one. The random walk noise component is in any case more difficult to be detected, since it asks for much longer time spans.

The temporally correlated noise that dominates GPS time-series can be adequately described as flicker noise, which is spatially correlated, and has a clear latitude dependence. Although the amplitude of the flicker noise has decreased in time since the first CGPS sites began producing data (early '90), it is still the dominant colored noise process (Williams *et al*., 2004). The vertical magnitudes are about 3 times larger than the horizontal ones.

In order to compute more realistic rate errors we adopt the approach of Mao *et al*., 1999, who developed an empirical model for estimating the GPS rate error (σ_r) for individual velocity components (north, east and vertical) using position time-series in presence of combined white and colored noise (flicker plus random walk). In our analysis we compute final rate errors using the formula:

$$\sigma_r^2 \cong \frac{12\sigma_w^2}{gT^3} + \frac{a\sigma_f^2}{g^b T^2} + \frac{\sigma_{rw}^2}{gT}$$

where g is the number of measurements per year, T is the total observation time span of observations (listed in Tab. 3), a and b are empiric constants, given in Mao *et al*., 1999 (a=1.78; b= 0.22). Noise magnitudes for white and flicker components, given in mm,

and for the random walk component, given in mm/√yr, have been computed considering the strong linear correlation observed by Mao *et al*., (1999) between the WRMS of GPS time-series and the corresponding white and flicker noise amplitudes. We use the WRMS obtained from the roust fit analysis of each individual position component and the linear relationship given by Dixon *et al*., 2000 to compute σ_w , σ_f and σ_{rw}.

Our choice of modeling the velocity errors as a function of white, flicker and random walk noise components, should provide over conservative uncertainties, but we presently prefer to be 10% more conservative than 500% optimistic (Mao *et al*., 1999).

5. DISCUSSION

We described the processing strategy used to analyze and combine CGPS observations collected at different networks in the Euro-Mediterranean region, with the aim of producing a self-consistent three dimensional velocity field suitable for geodynamics and tectonic applications. Caporali (2003), from the analysis of CGPS stations, found that the rates estimated from position time-series become stable after an observation window of at least three years. For this reason we only discuss results obtained from the analysis of the 31 sites of our data set that observed more than three years (see Tab.3).

The main product of our analysis is, for each station, a set of three dimensional position time-series, provided in a uniform and well defined global frame of reference (the ITRF2000). These time-series are used to compute horizontal and vertical velocities, assumed constant in time, and obtained trough a robust fit algorithm, which is less sensitive to the outliers and blunders present in the raw series, together with annual and semi-annual seasonal signals and epoch offsets. Although seasonal signals are in general quite small (at mm level), some stations display offsets as large as 9 cm (i.e., VENE). It is worth noting that larger offsets are usually observed in the vertical components, and are commonly due to changes in the GPS antenna configuration, as deduced by station log-files.

The mean values of post-fit WRSM for the north, east and vertical components (see Tab. 3) are about 1.7 mm, 1.8 mm and 4.8 mm, respectively. The station TGRC, in particular, is the worst site analyzed, displaying values of 2.08 mm, 3.28 mm and 7.24 mm in the three components as above, with a large data scatter, and an unclear seasonal signature (see Fig. 5c). In general, a model that considers also the seasonal terms

reduces the mean WRMS values by 4%, 3% and 6% for the north, east and vertical components, respectively.

The computed seasonal signals, listed in Tab. 3, and displayed in Fig. 5a, 5b, 5c and 5d only for some of the stations analyzed, are in average significantly below the 1 mm level for the horizontal components, whereas are larger than the 1 mm level in the vertical component.

The mean annual cosine and sine amplitudes for the north components are 0.55±0.06 mm and 0.39±0.06 mm, respectively, with the largest value observed at Venice (VENE: 2.40 mm) and Sarajevo (SRJV: 1.04 mm). The mean annual cosine and sine amplitudes for the east component are 0.66±0.08 mm and 0.39±0.08 mm, respectively, with the largest values observed at Rome (INGR: 2.58 mm) and Venice (VENE: 1.38 mm). The mean annual cosine and sine amplitudes for the vertical component are 2.79±0.20 mm and 1.06±0.21 mm, respectively, with largest values observed at Venice (VENE: 4.83 mm) and Osje (OSJE: 3.41 mm).

As regard the semi-annual terms, the mean cosine and sine amplitudes for the north component are 0.19±0.06 mm and 0.18±0.06 mm, respectively, with the largest values observed at Venice (VENE: 0.59 mm and 0.96 mm). The mean cosine and sine amplitudes for the east component are both 0.23±0.08 mm, with the largest values observed at Reggio Calabria (TGRC: 0.92 mm) and Venice (VENE:0.56 mm). The mean cosine and sine amplitudes for the vertical component are 0.57±0.20 mm and 0.53±0.20 mm, respectively, with the largest values observed at Castel del Monte (CADM: 1.61 mm) and Reggio Calabria (TGRC: 2.40 mm).

In our processing procedures we compute and remove the seasonal terms in order to reduce the daily data scatter and look at residual time-series, with the aim of improving the determination of the constant velocity term, which is the main goal of our analysis. Seasonal signals are generally related to: 1) gravitational excitation, 2) thermal origin coupled with hydrodynamics, 3) sources that are indirect due to geophysical processes, or of instrument, or modeling deficiency (Dong *et al*., 2002). The first category comprises rotational displacements due to seasonal polar motion (UT1), and loading induced displacement caused by solid Earth, ocean and atmospheric tides, which are modeled in the raw data reduction step (see section 5.1). However, residual ocean tide effects should still be present, and are mainly due to the use of global ocean tide models instead of higher quality local tidal models. Pole tide loading also belongs

to this first category, with the spectrum of mostly annual and Chandler wobble periods (~465 days). The deformation caused by pressure field variation, non-tidal sea surface fluctuation, ground water changes in both liquid and solid form, bedrock expansion beneath the GPS benchmark, and wind shear belong to the second category. The third category contains other error sources, which also generate apparent seasonal variations, such as orbit modeling errors caused by imperfect reference frame, which is defined through a set of stations that are subject to seasonal variations. There are other important phenomena that should affect the position time-series with a seasonal signatures; these involve tectonic-induced deformation, due to possible seasonal variations in regional fault slip or regional stress (e.g., slow earthquakes; Miller *et al.*, 2002), and this is one of the main reasons for which detecting non-tectonic signatures is a fundamental task. Table 5 provides the magnitudes of some individual sources that can potentially affect the GPS time-series (Dong *et al.*, 2002). Although most of the sources can be modeled and removed from the time-series (e.g., atmospheric mass loading, non-tidal mass loading, snow and soil moisture loading related effects) there is a set of complex sources that are much more difficult to asses and model. These includes: 1) neglected seasonal effects in the definition of the ITRF reference frame; 2) imperfect atmospheric modeling (Williams *et al*., 1998); 3) bedrock thermal expansion, which may affect the site vertical position at 0.5 mm level (Dong *et al*., 2002); 4) other environmental factors, including types of domes or monuments (Bock at al., 2000; Meertens *et al*., 1996; Hatanaka *et al*., 2001). Time independent antenna phase center model and multipath are also influenced by environmental factors, such as filling level of lakes, frozen/unfrozen of large water bodies, even tree trimming (King *et al*., 1995).

At different sites and networks different noise sources may dominate, and includes residual common mode positioning noise (white plus flicker noise), monument instabilities (random walk noise), and localized deformation due, for example, to changes in groundwater, or other non tectonic local loading. The spatially correlated common mode error (Wdowinsky *et al*., 1997), is removed, or at least significantly reduced, by performing the 7 parameters Helmert transformation, with regional stations included, and by removing annual and semi-annual signatures; this reduces by a factor of 2-3 the amplitudes of both white and flicker noise components, supporting Williams *et al*. (2004) explanation that a significant amount of the flicker noise is due to a common physical basis, with large spatial extend. The remaining flicker noise is

probably due to regional-scale processes such as atmospheric effects, and not to monument motions. Geodetic monument instability due to varying conditions of the anchoring media (e.g., soil, bedrock, building) is considered an important source of noise, thought to follow a random walk process (Johnson and Agnew, 1995; Langbein and Johnson, 1997). Whether or not the random walk noise is detectable depends on the length of the time-series, the sampling frequency, and the relative amplitudes of the other noise components. Random walk noise has been identified in continuous strain-meter data (Wyatt, 1982; Wyatt *et al*., 1989), and can be as high as 3 mm/√yr for some geodetic data (Johnson and Agnew, 1995). However, this type of disturbance can be mitigated by carefully designed monuments. The use of deeply anchored Wyatt design monuments (Wyatt *et al*., 1989; Bock *et al*., 1997), for example, provide an amplitude of only 0.4 mm/√yr (Johnson and Agnew, 2000). However, regional GPS networks have much longer inter-station spacing so that other sources of error, such as known random atmospheric propagation effects (Williams *et al*., 1998) could dominate the budget.

The network we analyze is realized through stations characterized by several different monument types (described in Tab.1). Pillars, or steel musts, anchored to stable buildings represent the largest number, while monuments directly founded on more and less consolidated bedrock are of different types: mainly concrete pillars, with some mast (i.e., VVLO) and tripod (i.e., TRO1). Since potential monument noise should be related to the stability of the monument itself with respect to potential local processes (i.e., soil humidity content and water table level changes, bedrock thermal expansion, etc), its constructive quality depends on how much the monument is able to reduce its response to those effects. However, we do not find any significant correlation between seasonal terms amplitudes and monument types. Stations realized through pillars founded directly on bedrock (e.g., AJAC, AQUI, CAGL, CAME, ELBA, GRAS, NOT1, ORID, VVLO) perform very well, with relatively lower amplitudes on both horizontal and vertical components. It is worth noting that also stations realized on buildings (e.g., BRAS, GENO, GRAZ, MATE, PRAT, UNPG) perform quite well, displaying horizontal seasonal amplitudes significantly below the 1 mm level. Only very bad monuments, like the one used for the station VENE, display very large amplitudes on both horizontal and vertical seasonal components. These observations, even if preliminary, are in agreement with results given by Williams *et al*., (2004), who analyzed noise characteristics of regional network solutions (in particular from the

SCIGN network in Southern California) to put some constraints on the quality of the different CGPS monuments involved. They found that deeply anchored Wyatt-designed monuments perform better that all other types, but also stations monumented on stable buildings are quite good, while the classic geodetic concrete pillars seem to perform indeed quite poorly.

To map our velocity solution into a reference frame that can be used for geo-kinematics interpretations of the study area, the horizontal ITRF velocities are rotated into a fixed Eurasian frame, and the vertical velocities are given with respect to an external stable frame (i.e., Sardinia-Corsica block or Central Europe). Figure 6a displays the residual velocities given with respect to the Eurasian fixed frame proposed by Serpelloni *et al.* (2005) of CGPS stations that observed for more than three years, ogether with velocities of CGPS stations that observed less than three years and non-permanent stations from Serpelloni *et al.* (2005). Vertical velocities are instead proposed with respect to a regionally stable external frame. In this work we used as stable area the Corsica-Sardinia region, which has been observed to be stable with respect to Eurasia both in terms of horizontal and vertical motions. Figure 6b displays the vertical rates, with one standard deviation errors, of CGPS stations that observed for more than three years.

6. CONCLUSIONS

We described the procedures routinely used to download, archive and analyze data from continuous GPS networks operating in the Mediterranean and European region, with the goal of deriving a self-consistent three dimensional velocity field that can be used for further geodynamics and geo-kinematics applications. The method used is based on a "distributed session" approach and provides several advantages, that can be summarized as following: 1) it makes an efficient use of computing resources; 2) it allows for the determination of a self-consistent set of station velocities in a uniform reference frame; 3) it allows for a rigorous combination among different space geodetic solutions; 4) it allows for a combination of continuous and campaign GPS observations into the same reference frame.

We performed an analysis of the position time-series for all the stations that observed for more than three years, with the aim of providing station velocities, together with the amplitudes of the annual and semi-annual signals and the offsets observed in

the series. The final result of our analysis is presented in terms of tables, reporting the velocity values and the amplitudes of the detected signals, and in terms of maps of horizontal and vertical velocities, given with respect to uniformly defined external stable frames.

Recent papers dealing with GPS observations in Italy and its surroundings revealed scientific problems about the kinematics and geodynamics of this region that will certainly benefit from the enlargement and improvement of the CGPS network, but that also require a multidisciplinary approach through the integration of seismological, geological and other geophysical and geodetic data (e.g., non-permanent networks, leveling measurements). In particular, the kinematics of Sicily with respect to Nubia (Africa), and its possible microplate-like behavior, is still matter of debate (Hollenstein *et al.*, 2003; D'Agostino and Selvaggi, 2004; Serpelloni *et al.*, 2005). In northeastern Sicily and Central Aeolian region large deformation rates and "anomalously" high horizontal velocities have been observed at non-permanent GPS stations (Hollenstein *et al*., 2003; Serpelloni *et al.*, 2005), and earthquake focal solutions reveal a rapid change in the seismotectonic setting east and west of the Salina-Lipari-Vulcano lineament (Pondrelli *et al*., 2004). Open questions for this area, which interests also the Messina Straits, involve the role of the Calabrian slab and the kinematics of the Ionian and Calabrian blocks, in the frame of a complex plate-boundary configuration (Goes *et al*., 2004). While upper bounds of active extension across the Apennines have been recently proposed (e.g., Hunstad *et al.*, 2003; Serpelloni *et al*., 2005), detailed information on how this deformation is distributed or localized across the active fault zones are still missing for most of the chain, and only dense non-permanent GPS networks are providing preliminary results (Anzidei *et al*., 2005). GPS data revealed the motion of the Adriatic block as independent, or partially independent, from the African plate (Battaglia *et al.*, 2004). However, Adria internal deformation and boundaries with respect to the African and Ionian domains are still unclear. At the same time, the possible presence of two partially independent Adriatic blocks is still matter of debate (Oldow et al., 2002; Battaglia *et al.*, 2004; D'Agostino *et al.*, 2005; Serpelloni *et al.*, 2005). The Northern Apennines and Po Plain region are still poorly understood from a kinematic point of view, also due to the low deformation rates involved (Serpelloni *et al.*, 2005), and the main goal of geodetic research in this region is to study where active

extensional and compressional strains are localized across the belt, toward the Po Plain and the Adriatic (http://earth.geology.yale.edu/RETREAT/).

The distributed processing mode adopted in this work allows us to look at the data collected at regional or local scale GPS networks, both permanent and non-permanent, from a global point of view, that is to include local or regional deformations (related for example to single fault segments) in a "plate tectonic" framework, with large advantages for a better comprehension of the tectonic and geodynamics processes that are deforming the crust in the Italian region.

Acknowledgments. This work was partially funded by the Italian Space Agency (ASI-ARS contract) and by Ministry of Public Education, University and Research. We are thankful to Prof. Enzo Boschi who supported this research. Thanks are due to ASI-CGS in Matera, Centro Ricerche Sismologiche of the Istituto Nazionale di Oceanografia e Geofisica Sperimentale in Udine, OLG Data Center, CNRS-UMR Géosciences Azur, and SOPAC for providing permanent GPS data and solutions. Thanks are also due to Prof. Alessandro Caporali (University of Padova), Dr. Mauro De Gasperi (Provincia Autonoma di Trento) and Dr. Marco Mucciarelli (Università della Basilicata), for making other RINEX data available. We are indebted with Dr. Danan Dong (JPL-Nasa) and Dr. Peng Fang (SOPAC- University of California) for stimulating discussions about GPS data analysis and for developing and making available the QOCA software. The maps were crated using the Generic Mapping Tools (GMT) software (Wessel and Smith, 1995).

REFERENCES

ABRAMOWITZ, M. and I.A. STEGUN, I. A. (Eds.) (1972): Handbook of Mathematical Functions with Formulas, Graphs, and Mathematical Tables, 9th printing. New York: Dover.

ALTAMINI, Z., P. SILLARD and C. BOUCHER (2002): ITRF2000: A new release of the International Terrestrial Reference Frame for earth science applications, *J. Geophys. Res.*, **107**(B10), 2214, doi:10.1029/2001JB000561.

ANZIDEI, M., P. BALDI, C. BONINI, G. CASULA, S. GANDOLFI and F. RIGUZZI (1998): Geodetic surveys across the Messina Straits (southern Italy) seismogenic area, *J. Geodyn.*, 25(2), 85-97.

ANZIDEI, M., P. BALDI, A. PESCI, A. ESPOSITO, A. GALVANI, F. LODDO, P. CRISTOFOLETTI, A. MASSUCCI and S. DEL MESE (2005): Geodetic deformation across the Central Apennines from GPS data in the time Span 1999-2003, *Ann. Geophys.*, 48(2), 259-271.

BATTAGLIA, M., M. MURRAY, E. SERPELLONI and R. BURGMANN (2004): The Adriatic region: an independent microplate within the Africa-Eurasia collision zone, *Geophys. Res. Lett.*, **31**, L09605, doi:10.1029/2004GL019723 .

BLEWITT, G., Y. BOCK and G. GENDT (1993): Regional clusters and distributed processing, *IGS Analysis Center Workshop*, Ottawa, Canada, pp. 62-91.

BOCK, Y., S.A. GOUREVITCH, C.C. COUNSELMAN III, R.W. KING, R.W. and R.I. ABBOT (1986): Interferometric analysis of GPS phase observations, *Manuscripta Geodetica*, **11**, 282-288.

BOCK, Y., S. WDOWINSKI, P. FANG, J. ZHANG, S. WILLIAMS, H. JOHNSON, J. BEHR, J. GENRICH, J. DEAN, M. VAN DOMSELAAR, D. AGNEW, F. WYATT, K. STARK, B. ORAL, K. HUDNUT, R.W. KING, T.H. HERRING, S. DINARDO, W. YOUNG, D. JACKSON and W. GURTNER, W. (1997): Southern California Permanent GPS Geodetic Array: Continuous measurements of regional crustal deformation between the 1992 Landers and 1994 Northridge earthquakes, *J. Geophys. Res.*, **102**(B8), 18013-18034, 10.1029/97JB01379.

BOCK, Y., R.M. NIKOLAIDIS, P.J. DE JONGE and M.. BEVIS, M. (2000): Instantaneous geodetic positioning at medium distances with the Global

Positioning System, *J. Geophys. Res.*, **105**(B12), 28223-28254, 10.1029/2000JB900268.

CALAIS, E., R. BAYER, J. CHÉRY, F. COTTON, M. FLOUZAT, F. JOUANNE, J. MARTINOD, F. MATHIEU, O. SCOTTI, M. TARDY and C. VIGNY (2000): REGAL: A permanent GPS network in the French Western Alps, Configuration and first results, *C.R. Acad. Sci. Paris,* **331**, 435-442.

CAPORALI, A. (2003): Average strain rate in the Italian crust inferred from a permanent GPS network – I. Statistical analysis of the time-series of permanent stations, *Geophys. J. Int.*, **155**, 241-253.

D'AGOSTINO, N. and G. SELVAGGI (2004): Crustal motion along the Eurasia-Nubia plate-boundary in the Calabrian Arc and Sicily and active extension in the Messina Straits from GPS measurements, *J. Geophys. Res.*, **109**, B11402, doi:10.1029/2004JB002998.

D'AGOSTINO, N., D. CHELONI, S. MANTENUTO, G. SELVAGGI, A. MICHELINI and D. ZULIANI (2005): Strain accumulation in the southern Alps (NE Italy) and deformation at the northeastern boundary of Adria observed by CGPS measurements, *Geophys. Res. Lett.*, **32**, L19306, doi:10.1029/2005GL024266.

DING, X.L., D.W. ZHENG, D.N. DONG, C. MA, Y.Q. CHEN and G.L. WANG (2005). Seasonal and secular positional variations at eight co-located GPS and VLBI stations, *Journal of Geodesy*, **79**, Issue 1 - 3, 71 – 81.

DIXON, T.H., M. MILLER, F. FARINA, H. WANG and D. JOHNSON (2000): Present-day motion of the Sierra Nevada block and some tectonic implications for the Basin and Range province, North American Cordillera, *Tectonics*, **19**(1), 1-24.

DONG, D. and Y. BOCK (1989): Global Positioning System network analysis with phase ambiguity resolution applied to crustal deformation studies in California, *J. Geophys. Res.*, **94**, 3949-3966.

DONG, D., T.A. HERRING and R.W. KING (1998): Estimating regional deformation from a combination of space and terrestrial geodetic data, *J. Geod.*, **72**, 200-214.

DONG, D., P. FANG, Y. BOCK, M.K. CHENG and S. MIYAZAKI (2002): Anatomy of apparent seasonal variation from GPS–derived site position, *J. Geophys. Res.*, **107**, 10.1029/2001JB000573.

GOES, S., D. GIARDINI, S. JENNY, C. HOLLENSTEIN, H.G. KHALE and A. GEIGER (2004): A recent tectonic reorganization in the south-central Mediterranean, *Earth. Planet. Scie. Lett.*, **226**, 335-345.

HATANAKA, Y., M. SAWADA, A. HORITA, M. KUSAKA, J. JOHNSON and C. ROCKEN (2001): Calibration of antenna-radome and monument-multipath effect on GEONET – Part2: evaluation of the phase map by GEONET data, *Earth, Planets and Space*, **53**, 23-30.

HEFLIN, M., W. BERTIGER, G. BLEWITT, A. FREEDMAN, K. HURST, S. LICHTEN, U. LINDQUISTER, Y. VIGUE, F. WEBB, T. YUNCK and J. ZUMBERGE (1992): Global geodesy using GPS without fiducial sites, *Geophys. Res. Lett.*, **19**, 131-134.

HERRING, T.H., J.L. DAVIS and I.I. SHAPIRO (1990): Geodesy by radio interferometry: The application of Kalman filtering to the analysis of very long baseline interferometry data, *J. Geophys. Res.*, **95**(B8), 12561-12581, 10.1029/90JB00683.

HERRING, T.H., D. DONG and R.W. KING (1991): Sub-milliarcsecond determination of pole position using the Global Positioning System, *Geophys. Res. Lett.*, **18**, 1893-1896.

HERRING, T.A. (2000): GLOBK: Global Kalman filter VLBI and GPS analysis program Version 10.0, Massachusetts Institute of Technology, Cambridge.

HOLLENSTEIN, CH., H.G. KAHLE, A. GEIGER, S. JENNY, S. GOES and D. GIARDINI (2003): New GPS constraints on the Africa-Eurasia plate-boundary zone in southern Italy, *Geophys. Res. Lett.*, **30**(18), 1935, doi:10.1029/2003GL017554.

HUNSTAD, I., G. SELVAGGI, N. D'AGOSTINO, P. ENGLAND, P. CLARKE and M. PIEROZZI (2003): Geodetic strain in peninsular Italy between 1875 and 2001, *Geophys. Res. Lett.*, **30(4)**, 1181,doi:10.1029/2002GL016447.

JOHNSON, H. and D. AGNEW (1995): Monument motion and measurements of crustal velocities, *Geophys. Res. Lett.*, **22**, 2905-2908.

JOHNSON, H. and D. AGNEW (2000): Correlated noise in geodetic time series, *U.S. Geol. Surv., Final tech. Rep.*, FTR-1434-HQ-97-GR-03155.

KING, N. E., J.L. SVARC, E.B. FOGLEMAN, W.K. GROSS, K.W. CLARK, G.D. HAMILTON, C.H. STIFFLER and J.M. SUTTON (1995): Continuous GPS

observations across the Hayward fault, California, 1991 - 1994, *J. Geophys. Res.*, **100**(B10), 20271-20284, 10.1029/95JB02035.

KING, R.W., J. COLLINS, E.M. MASTERS, C. RIZOS and A. STOLZ (1985): *Surveying with Global Positioning System, Monograph No. 9*, School of Surveying, University of New South Wales, Sydney.

KING, R.W. and Y. BOCK (2000): Documentation for GAMIT GPS analysis software, version 10.01, Massachusetts Institute of Technology and Scripps Institution of Oceanography.

LANGBEIN, J. and H. JOHNSON (1997): Correlated errors in geodetic time series: Implications for time-dependent deformation, *J. Geophys. Res.*, **102**, 591-603.

LARSON, K.M., J.T. FREYMUELLER and S. PHILIPSEN (1997): Global plate velocities from the Global Positioning System, *J. Geophys. Res.*, **102**, 591–603.

MAO, A., C.G.A. HARRISON and T.H. DIXON (1999): Noise in GPS coordinate time series, *J. Geophys. Res.*, **104**, 2797-2816.

MCCARTHY, D.D. (Ed.) (1996): IERS Conventions 1996, *IERS Tech. Note 21, Int. Earth Rotations Serv.*, Obs. de Paris.

MCCLUSKY, S., R. REILINGER, S. MAHMOUD, D. BEN SARI and A. TEALEB (2003): GPS constraints on Africa (Nubia) and Arabia plate motions, *Geophys. J. Int.*, **155**, 126-138.

MEERTENS, C., C. ALBER, J. BRAUN, C. ROCKEN, B. STEPHENS, R. WARE, M. EXNER and P. KOLESNIKOFF (1996): Field and anechoic chamber tests of GPS antennas, *Proceedings of IGS analysis center workshop, Silver Springs, MD, U.S.A., June 1996*, International GPS Service, 107-118.

MILLER, M.M., T. MELBOURNE, D.J. JOHNSON and W.Q. SUMNER (2002): Periodic Slow Earthquakes from the Cascadia Subduction Zone, *Science*, **295**, no. 5564, 2423.

NOCQUET, J.M. and E. CALAIS (2003): Crustal velocity field of western Europe from permanent GPS array solutions, 1996-2001, *Geophys. J. Int.*, **154**, 72-88.

OLDOW, J.S., L. FERRANTI, D.S. LEWIS, J.K. CAMPBELL, B. D'ARGENIO, R. CATALANO, G. PAPPONE, L. CARMIGNANI, P. CONTI and C.L.V. AIKEN (2002): Active fragmentation of Adria, the North African promontory, central Mediterranean Orogen, *Geology*, 30(9), 779-782.

PONDRELLI, S., C. PIROMALLO and E. SERPELLONI (2004): Convergence vs. Retreat in Southern Tyrrhenian Sea: insights from kinematics, Geophys. Res. Lett., **31**, L0661, doi:10.1029/2003GL019223.

SANSÒ, F. and M.C. DE LACY (2000): Uno studio sulle diverse applicazioni del GPS e sul futuro sviluppo della rete di stazioni permanenti GPS sul territorio italiano orientato alla creazione di un servizio geodetico nazionale, *available at* http://geomatica.como.polimi.it/gps/articoli/asi.pdf.

SCHAFFRIN, B. and Y. BOCK (1988): A unified scheme for processing GPS dual-band phase observations, *Bull. Géod.*, **62**, 142-160.

SCHERNECK, H.G. (1991): A parameterized solid Earth tide model and ocean tide loading effects for global geodetic baseline measurements, *Geophys. J. Int.*, **106**, 677-694.

SERPELLONI, E., M. ANZIDEI, P. BALDI, G. CASULA, A. GALVANI, A. PESCI and F. RIGUZZI (2002): Combination of permanent and non-permanent GPS networks for the evaluation of the strain-rate field in the central Mediterranean area, *Boll. Geofis. Teor. Appl.*, **43**, 195-219.

SERPELLONI, E., M. ANZIDEI, P. BALDI, G. CASULA and A. GALVANI (2005): Crustal velocity and strain-rate fields in Italy and surrounding regions: new results from the analysis of permanent and non-permanent GPS networks, *Geophy. J. Int.*, **161**(3), 861-880. doi:10.1111/j.1365-246X.2005.02618.x.

WDOWINKSKI, S., Y. BOCK, J. ZHANG, P. FANG and J. GENRICH (1997): Southern California permanent GPS geodetic array: Spatial filtering of daily positions for estimating coseismic and postseismic displacements induced by the 1992 Landers earthquake, *J. Geophys. Res.*, **102**(B8), 18057-18070, 10.1029/97JB01378.

WESSEL, P. and W.H.F. SMITH (1995): New Version of the Generic Mapping Tools Released, *EOS Trans.*, **76**, 329.

WILLIAMS, S., Y. BOCK and P. FANG, P. (1998): Integrated satellite interferometry: Tropospheric noise, GPS estimates and implications for interferometric synthetic aperture radar products, *J. Geophys. Res.*, **103**(B11), 27051-27068, 10.1029/98JB02794.

WILLIAMS S.D.P., Y. BOCK, P. FANG, P. JAMASON, R.M. NIKOLAIDIS, L. PRAWIRODIRDJO, M. MILLER and D.J. JOHNSON (2004): Error analysis of

continuous GPS position time series, *J. Geophys. Res.*, **109**, B03412, doi:10.1029/2003JB002741.

WYATT, F.K. (1982). Displacement of Surface Monuments: Horizontal Motion, *J. Geophys. Res.*, **87**, 979-989.

WYATT, F.K., H. BOLTON, S. BRALLA and D. AGNEW (1989): New designs of geodetic monuments for use with GPS, *Eos. Trans. AGU*, 70, 1054.

ZHANG, J., Y. BOCK, H. JOHNSON, P. FANG, S. WILLIAMS, J. GENRICH, S. WDOWINSKI and J. BEHR (1997): Southern California permanent GPS geodetic array: Error analysis of daily position estimates and site velocities, *J. Geophys. Res.*, **102**, 18.035-18.055.

TABLE CAPTIONS

Table 1. List of the Continuous GPS stations archived and analyzed in this work. Columns from left to right display: station number, full name, longitude, latitude, four character ID, network to which the station formally belongs (IGS = International GPS Service network; EUREF: EUropean REFerence network; ASI: Agenzia Spaziale Italiana network; FREDNET: FRiuli REgional Deformation NETwork; INGV: Istituto Nazionale di Geofisica e Vulcanologia network; REGAL: REseau GPS permanent dans les ALpes network; AUSTRIA: Austrian GPS network; OTHER: other stations not belonging to any specific network), remote ftp archive addresses for data downloading, source for the equipment changes information (*sopac*: from SOPAC *station.info* file; *epn*: from EUREF station history file; *log*: from station log file; *rnx*: from RINEX file header), number referring to the cluster in which the station is processed (1: southern cluster, 2: northern cluster; 3: mixed cluster), station monument descriptions.

Table 2. List and coordinates of the 50 global and regional tracking stations used to apply the internal constraints in the reference frame definition.

Table 3. Amplitudes of the annual, semi-annual signals and offsets detected from the analysis of position time-series of stations that observed more than 3 years. For each station (ID code), the observation interval (ΔT), the annual and semiannual cosine and sine amplitudes (in mm), the weighted RMS, the epochs of breaks in the time-series and the related offsets are listed for the north, east and vertical components. One standard deviation errors are also given.

Table 4. Velocity values and 1σ uncertainties for the CGPS stations that observed for more than three years. Residual horizontal velocities are given with respect to the Eurasian frame of Serpelloni et al. (2005), and residual vertical velocities are given with respect to the Corsica.Sardinia block.

Table 5. Contributions of geophysical sources and model errors to the observed annual and semiannual variations in site positions.

FIGURE CAPTIONS

Figure 1a. Euro-Mediterranean map showing the distribution of the CGPS stations archived, processed and discussed in this work. The names of the IGS stations used are also displayed.

Figure 1b. Central Mediterranean map showing the distribution and names (4 character ID code), of the CGPS stations archived, processed and discussed in this work.

Figure 2. Flow chart of the CGPS data archiving procedures.

Figure 3. Flow chart of the CGPS data processing steps.

Figure 4a, b. Maps of the whole combined CGPS network that is obtained from the combination of out three regional solutions with the SOPAC loosely constrained solutions. Position time-series, and three dimensional velocities, are available for all the stations displayed.

Figure 5a, b, c, and d. Position time-series (after removing the constant velocity) of the Italian stations that observed for more than 3 years. The red error bars represent 1 standard deviation formal uncertainties obtained from the GAMIT/GLOBK analysis. Annual and semiannual signals are also displayed, with uncertainties (red curve). Dotted black lines show the epochs of the significant offsets in the time-series that have been computed and corrected (epochs and offsets values are listed in Tab. 3).

Figure 6a. Residual velocities (in mm/yr), and 95% error ellipses, given with respect to the stable Eurasian frame described in Serpelloni *et al*. (2005). Red arrows: velocities of CGPS stations that observed fro more than three years; yellow arrows: velocities for CGPS stations that observed for less than three years; white arrows: velocities from non-permanent stations surveyed in the 1991-2004 time span (Serpelloni *et al.*, 2005).

Figure 6b. Residual vertical velocities (in mm/yr), with one standard deviation error bars, given with respect to the stable Corsica-Sardinia block. Numbers are given only for stations showing significant vertical rates.

N°	Station Name	Lon.	Lat.	ID	Net	FTP archive	Stinfo	SN	Monument type
1	Ankara	32.75	39.88	**ANKR**	IGS	ftp://lox.ucsd.edu/pub/rinex/yyyy/ddd	*sopac*	1,2,3	Pillar on weathered bedrock (limestone)
2	Cagliari	8.97	39.13	**CAGL**	IGS	ftp://lox.ucsd.edu/pub/rinex/yyyy/ddd	*sopac*	1,2,3	Pillar on igneous bedrock
3	Herstmonceaux	0.33	50.87	**HERS**	IGS	ftp://lox.ucsd.edu/pub/rinex/yyyy/ddd	*sopac*	1,2,3	8 m height steel mast on unconsolidated soils
4	Kootwijk	5.81	52.18	**KOSG**	IGS	ftp://lox.ucsd.edu/pub/rinex/yyyy/ddd	*sopac*	1,2,3	-
5	Madrid	-4.25	40.43	**MAD2**	IGS	ftp://lox.ucsd.edu/pub/rinex/yyyy/ddd	*sopac*	1,2,3	Brass disk on roof of building founded on unconsolidated soils (sands)
6	Mas Palomas	-15.63	27.76	**MAS1**	IGS	ftp://lox.ucsd.edu/pub/rinex/yyyy/ddd	*sopac*	1,2,3	Pillar on bedrock
7	Matera	16.70	40.65	**MATE**	IGS	ftp://lox.ucsd.edu/pub/rinex/yyyy/ddd	*sopac*	1,2,3	Pillar on roof of building founded on sedimentary bedrock
8	Potsdam	13.06	52.38	**POTS**	IGS	ftp://lox.ucsd.edu/pub/rinex/yyyy/ddd	*sopac*	1,2,3	Pillar on building founded on sediments
9	Tromso	18.94	69.66	**TRO1**	IGS	ftp://lox.ucsd.edu/pub/rinex/yyyy/ddd	*sopac*	1,2,3	5.5 m steel mast on fresh sedimentary/metamorphic bedrock
10	Wettzell	12.88	49.14	**WTZR**	IGS	ftp://lox.ucsd.edu/pub/rinex/yyyy/ddd	*sopac*	1,2,3	Steel plate on concrete tower founded on weathered igneous bedrock
11	Zwen Astronomical	36.75	55.69	**ZWEN**	IGS	ftp://lox.ucsd.edu/pub/rinex/yyyy/ddd	*sopac*	1,2,3	Pillar on the roof of building
12	Ajaccio	8.76	41.93	**AJAC**	EUREF	ftp://igs.ifag.de/EUREF/obs/year/doy	*sopac*	1	Reinforced concrete pillar on igneous bedrock
13	Aquila	13.35	42.37	**AQUI**	EUREF	ftp://igs.ifag.de/EUREF/obs/year/doy	*sopac*	1	Pillar on sedimentary bedrock
14	Bolzano	11.34	46.49	**BZRG**	EUREF	ftp://igs.ifag.de/EUREF/obs/year/doy	*sopac*	2	Steel pillar on the roof of building
15	Camerino	13.12	43.11	**CAME**	EUREF	ftp://igs.ifag.de/EUREF/obs/year/doy	*sopac*	1	Pillar on sedimentary bedrock
16	Como	9.09	45.80	**COMO**	EUREF	ftp://geodaf.mt.asi.it/GEOD/GPSD/RAW/yyyy/ddd	*log*	2	Stable pillar on roof of building founded on fresh sedimentary bedrock (sand/clays)
17	Dubrovnic	18.11	42.65	**DUBR**	EUREF	ftp://igs.ifag.de/EUREF/obs/year/doy	*epn*	1	Steel tripod anchored to flat roof of building founded on weathered sedimentary bedrock
18	Elba	10.21	42.75	**ELBA**	EUREF	ftp://igs.ifag.de/EUREF/obs/year/doy	*epn*	1	Stable pillar on bedrock
19	Genova	8.92	44.42	**GENO**	EUREF	ftp://igs.ifag.de/EUREF/obs/year/doy	*sopac*	2	Pillar on the roof of building founded on folded sedimentary bedrock
20	Geoservis GS-REF1	14.54	46.05	**GSR1**	EUREF	ftp://igs.ifag.de/EUREF/obs/year/doy	*epn*	2	1.5 m steel mast on the top of building
21	Lampedusa	12.60	35.50	**LAMP**	EUREF	ftp://igs.ifag.de/EUREF/obs/year/doy	*sopac*	1	Steel mast on the roof of building
22	La Palma	-17.32	28.27	**LPAL**	EUREF	ftp://igs.ifag.de/EUREF/obs/year/doy	*epn*	1	Reinforced concrete pillar on the top of roof of a 3 m height building founded on bedrock
23	Marsiglia	5.35	43.28	**MARS**	EUREF	ftp://igs.ifag.de/EUREF/obs/year/doy	*sopac*	2	Aluminum plate on the terrace of building founded on sedimentary bedrock (clays)
24	Noto	14.99	36.87	**NOT1**	EUREF	ftp://lox.ucsd.edu/pub/rinex/yyyy/ddd	*sopac*	1,2,3	Concrete pillar founded on sedimentary bedrock
25	Oberpfaffenhofen	11.18	48.06	**OBE2**	EUREF	ftp://igs.ifag.de/EUREF/obs/year/doy	*sopac*	2	2.51 m height steel mast on the roof of building
26	Ohrid	20.79	41.12	**ORID**	EUREF	ftp://igs.ifag.de/EUREF/obs/year/doy	*sopac*	1	Concrete pillar on jointed sedimentary bedrock
27	Oroshaza	20.40	46.33	**OROS**	EUREF	ftp://igs.ifag.de/EUREF/obs/year/doy	*epn*	1	Forced centered marker tied on an unused chimney founded on weathered sedimentary bedrock
28	Osijec	18.68	45.56	**OSJE**	EUREF	ftp://igs.ifag.de/EUREF/obs/year/doy	*sopac*	1	1 m height steel mast anchored on the wall of roof on weathered sedimentary bedrock
29	Padova	11.89	45.41	**PADO**	EUREF	ftp://lox.ucsd.edu/pub/rinex/yyyy/ddd	*sopac*	1,2,3	Steel plate on the roof of building founded on sedimentary bedrock (clay/sand)
30	Penc	19.28	47.78	**PENC**	EUREF	ftp://lox.ucsd.edu/pub/rinex/yyyy/ddd	*sopac*	2	Concrete pillar on the roof of building founded on stable sedimentary bedrock
31	Pfaender	9.78	47.51	**PFAN**	EUREF	ftp://igs.ifag.de/EUREF/obs/year/doy	*sopac*	2	2 m steel mast on fresh sedimentary bedrock
32	Prato	11.09	43.88	**PRAT**	EUREF	ftp://geodaf.mt.asi.it/GEOD/GPSD/RAW/yyyy/ddd	*sopac*	2	Concrete pillar on roof of building founded on sedimentary (send/gravel) bedrock
33	Saint Jean des Vignes	4.67	45.88	**SJDV**	EUREF	ftp://igs.ifag.de/EUREF/obs/year/doy	*sopac*	2	Steel mast on top of small concrete building directly anchored into bedrock (limestone)
34	Saraievo	18.41	43.87	**SRJV**	EUREF	ftp://igs.ifag.de/EUREF/obs/year/doy	*sopac*	1	Steel mast on chimney of stable building
35	Torino	7.66	45.06	**TORI**	EUREF	ftp://igs.ifag.de/EUREF/obs/year/doy	*sopac*	1,2,3	Steel mast at top of wall on stable building founded on sediments

36	Perugia	12.35	43.12	**UNPG**	EUREF	ftp://igs.ifag.de/EUREF/obs/year/doy	*sopac*	1	Stale concrete pillar on top of roof of building founded on jointed sedimentary (fluvial) bedrock
37	Brescia	10.23	45.55	**BRIX**	ASI	ftp://geodaf.mt.asi.it/GEOD/GPSD/RAW/yyyy/ddd	*log*	2	Pillar on roof of building founded on sediments (sand/gravel)
38	Cosenza	16.31	39.20	**COSE**	ASI	ftp://geodaf.mt.asi.it/GEOD/GPSD/RAW/yyyy/ddd	*sopac*	3	Stable pillar on the roof of building founded on fresh metamorphic bedrock
39	ING-Roma	12.51	41.83	**INGR**	ASI	ftp://geodaf.mt.asi.it/GEOD/GPSD/RAW/yyyy/ddd	*log*	1	Stable pillar on roof of building founded on not fractured piroclastic bedrock
40	Lecco	9.24	45.51	**LEC1**	ASI	ftp://geodaf.mt.asi.it/GEOD/GPSD/RAW/yyyy/ddd	*log*	3	Stable pillar on roof of building founded on sedimentary bedrock (sand/gravel)
41	Maratea	15.69	40.00	**MARA**	ASI	ftp://geodaf.mt.asi.it/GEOD/GPSD/RAW/yyyy/ddd	*log*	1	Stable pillar on roof of building founded on jointed sedimentary bedrock
42	Milo (Trapani)	12.58	38.01	**MILO**	ASI	ftp://geodaf.mt.asi.it/GEOD/GPSD/RAW/yyyy/ddd	*log*	1	Stable concrete pillar founded on sedimentary bedrock
43	Novara	8.61	45.44	**NOVA**	ASI	ftp://geodaf.mt.asi.it/GEOD/GPSD/RAW/yyyy/ddd	*sopac*	1	-
44	Palma Campania	14.33	40.52	**PACA**	ASI	ftp://geodaf.mt.asi.it/GEOD/GPSD/RAW/yyyy/ddd	*log*	1	Stable iron pillar on the roof of building founded on sedimentary bedrock
45	Pavia	9.13	45.20	**PAVI**	ASI	ftp://geodaf.mt.asi.it/GEOD/GPSD/RAW/yyyy/ddd	*rnx*	2	-
46	Reggio Calabria	15.64	38.11	**TGRC**	ASI	ftp://geodaf.mt.asi.it/GEOD/GPSD/RAW/yyyy/ddd	*log*	1	Stable pillar on roof of building
47	Tito Scalo	15.72	40.60	**TITO**	ASI	ftp://geodaf.mt.asi.it/GEOD/GPSD/RAW/yyyy/ddd	*log*	1	Stable pillar on roof of building founded on shale
48	Ferrara	11.60	44.83	**UNFE**	ASI	ftp://geodaf.mt.asi.it/GEOD/GPSD/RAW/yyyy/ddd	*sopac*	2	Metallic pillar on the roof of building founded on alluvial sends
49	Vallo della Lucania	15.26	40.23	**VLUC**	ASI	ftp://geodaf.mt.asi.it/GEOD/GPSD/RAW/yyyy/ddd	*sopac*	1	Stable pillar on the roof of building
50	Monte Acomizza	13.52	46.55	**ACOM**	FREDNET	ftp://wave.crs.inogs.it/pub/gps/rinex/yyyy/ddd	*sopac*	2	Concrete reinforced pillar founded on fresh bedrock (limestone)
51	Alpe Faloria	12.18	46.53	**AFAL**	FREDNET	ftp://wave.crs.inogs.it/pub/gps/rinex/yyyy/ddd	*sopac*	2	Concrete reinforced pillar founded on fresh bedrock (limestone)
52	Caneva	12.43	46.00	**CANV**	FREDNET	ftp://wave.crs.inogs.it/pub/gps/rinex/yyyy/ddd	*sopac*	2	Concrete reinforced pillar founded on fresh bedrock (limestone)
53	Colle di Medea	13.44	45.92	**MDEA**	FREDNET	ftp://wave.crs.inogs.it/pub/gps/rinex/yyyy/ddd	*sopac*	2	Concrete reinforced pillar founded on fresh bedrock (limestone)
54	Mont di Prat	12.99	46.24	**MPRA**	FREDNET	ftp://wave.crs.inogs.it/pub/gps/rinex/yyyy/ddd	*sopac*	2	Concrete reinforced pillar founded on fresh bedrock (limestone)
55	Trieste	13.76	45.71	**TRIE**	FREDNET	ftp://wave.crs.inogs.it/pub/gps/rinex/yyyy/ddd	*sopac*	2	Steel mast anchored to the wall of building
56	Zouf	12.58	46.33	**ZOUF**	FREDNET	ftp://wave.crs.inogs.it/pub/gps/rinex/yyyy/ddd	*sopac*	2	Concrete reinforced pillar founded on fresh bedrock (limestone)
57	Brasimone	11.11	44.12	**BRAS**	INGV/UNIBO	ftp://lox.ucsd.edu/pub/rinex/yyyy/ddd	*sopac*	1,2,3	Concrete block on roof of building
58	Gibilmanna	14.03	37.98	**GBLM**	INGV	CONV	*log*	1	Concrete pillar on bedrock
59	Preturo	13.32	42.38	**INGP**	INGV	LOCAL	*log*	3	Concrete pillar on bedrock
60	Roseto degli Abruzzi	14.00	42.65	**RSTO**	INGV	CONV	*log*	3	Concrete pillar founded on sediments
61	Teolo	11.70	45.37	**TEOL**	INGV	CONV	*log*	2	Concrete reinforced pillar on jointed bedrock
62	Villa Valle Longa	13.62	41.87	**VVLO**	INGV	CONV	*log*	3	Steel mast on sedimentary bedrock (limestone)
63	Chatel de Joux	5.78	46.52	**JOUX**	REGAL	ftp://kreiz.unice.fr/pub/Regal/serrurier/yyyy	*log*	2	Concrete pillar on fresh sedimentary bedrock
64	La Feclaz	5.98	45.63	**FCLZ**	REGAL	ftp://kreiz.unice.fr/pub/Regal/yyyy	*log*	2	Concrete pillar on fresh sedimentary bedrock
65	Saint Michel l'Obs.	5.72	43.92	**MICH**	REGAL	ftp://lareg.ensg.ign.fr/pub/rgp/yyyy/ddd	*log*	2	Concrete pillar on fresh sedimentary bedrock
66	Modane	6.70	45.20	**MODA**	REGAL	ftp://lareg.ensg.ign.fr/pub/rgp/yyyy/ddd	*log*	2	Antenna fixed on top of concrete platform anchored into fresh metamorphic bedrock
67	Le Sauvan	4.47	44.25	**SAUV**	REGAL	ftp://kreiz.unice.fr/pub/Regal/yyyy	*log*	2	Concrete pillar on fresh sedimentary bedrock
68	Saint Vèran	6.90	44.68	**SVRN**	REGAL	ftp://kreiz.unice.fr/pub/Regal/yyyy	*log*	2	Concrete pillar on fresh bedrock

69	Welschbruch	7.35	48.40	**WELS**	REGAL	ftp://kreiz.unice.fr/pub/Regal/yyyy	*log*	2	-
70	Patscherkofel	11.47	47.20	**PATK**	AUSTRIA	ftp://olggps.oeaw.ac.at/pub/outdata/patk	*rnx*	2	Concrete pillar and steel mast anchored on granite bedrock
71	Rottenmann	14.35	47.52	**RTMN**	AUSTRIA	ftp://olggps.oeaw.ac.at/pub/outdata/rtmn	*rnx*	2	Concrete pillar and steel mast on roof of building
72	Salzburg	13.12	47.80	**SBGZ**	AUSTRIA	ftp://igs.ifag.de/EUREF/obs/year/doy	*sopac*	2	Concrete pillar and steel mast anchored on sedimentary bedrock
73	Villach	13.87	46.60	**VLCH**	AUSTRIA	ftp://olggps.oeaw.ac.at/pub/outdata/vlch	*rnx*	2	-
74	Vienna	16.38	48.22	**WIEN**	AUSTRIA	ftp://olggps.oeaw.ac.at/pub/outdata/wien	*rnx*	2	Steel mast on roof of building
75	Asiago	11.53	45.85	**ASIA**	OTHER	CONV	*rnx*	2	-
76	Basovizza	13.85	45.63	**BASO**	OTHER	LOCAL	*log*	3	Concrete block on bedrock
77	Castel del Monte	16.27	41.07	**CADM**	OTHER	CONV	*log*	3	Pillar on roof of building
78	Merano	11.17	46.67	**MERA**	OTHER	CONV	*rnx*	3	-
79	Rovereto	11.04	45.89	**ROVE**	OTHER	CONV	*rnx*	3	-
80	Rovigo	11.79	45.07	**ROVI**	OTHER	CONV	*rnx*	2	-
81	Trento	11.07	46.04	**TREN**	OTHER	CONV	*rnx*	3	Steel mast on roof of building

Tab. 1a

Station	Lon	Lat	Station	Lon	Lat	Station	Lon	Lat	Station	Lon	Lat	Station	Lon	Lat
ALBH	-123.49	48.39	GRAS	6.92	43.76	MAC1	158.94	-54.50	PERT	115.89	-31.80	TRO1	18.9	69.7
ALGO	-78.07	45.96	GRAZ	15.49	47.07	MALI	40.19	-3.00	PIE1	-108.12	34.30	TSKB	140.1	36.1
BOR1	17.07	52.28	GUAM	144.87	13.59	MAS1	-15.63	27.76	POTS	13.07	52.38	USUD	138.4	36.1
BRMU	-64.70	32.37	HARK	27.71	-25.89	MATE	16.70	40.65	REYK	-21.96	64.14	VILL	-4.0	40.4
BRUS	4.36	50.80	HERS	0.34	50.87	MDO1	-104.02	30.68	SHAO	121.20	31.10	WES2	-71.5	42.6
CAGL	8.97	39.14	IRKT	104.32	52.22	METS	24.40	60.22	STJO	-52.68	47.60	WETT	12.9	49.1
DAV1	77.97	-68.58	JOZE	21.03	52.10	NLIB	-91.58	41.77	TELA	34.78	32.07	WTZR	12.9	49.1
DRAO	-119.63	49.32	KERG	70.26	-49.35	NYAL	11.87	78.93	TIDB	148.98	-35.40	YAR1	115.3	-29.0
FORT	-38.43	-3.88	KOKB	-159.67	22.13	NYA1	11.87	78.93	TOUL	1.48	43.56	YELL	-114.5	62.5
GOLD	-116.89	35.43	KWJ1	167.73	8.72	ONSA	11.93	57.40	TROM	18.94	69.66	ZIMM	7.5	46.9

Tab. 2

Station name	Component	Annual Cos (mm)	Annual Sin (mm)	Semiannual Cos (mm)	Semiannual Sin (mm)	WRMS mm	Offsets					
							d/m/y	mm	d/m/y	mm	d/m/y	mm
AJAC	North	0.40 ± 0.06	0.77 ± 0.06	-0.07 ± 0.06	-0.63 ± 0.06	1.43						
ΔT (yrs)	East	-0.34 ± 0.08	-0.07 ± 0.08	0.33 ± 0.08	-0.10 ± 0.08	1.86						
3.3648	Up	-2.08 ± 0.18	1.63 ± 0.17	0.21 ± 0.17	-0.33 ± 0.17	4.09						
AQUI	North	0.19 ± 0.06	0.79 ± 0.07	-0.02 ± 0.07	-0.25 ± 0.06	1.77	27/08/2001	0.76 ± 0.17				
ΔT (yrs)	East	-0.56 ± 0.08	0.67 ± 0.08	0.40 ± 0.08	-0.21 ± 0.07	2.02	27/08/2001	3.75 ± 0.21				
4.547	Up	-3.00 ± 0.21	-1.12 ± 0.21	0.41 ± 0.21	1.03 ± 0.20	5.6	27/08/2001	-7.40 ± 0.54				
BRAS	North	-0.18 ± 0.07	-0.32 ± 0.07	-0.04 ± 0.07	-0.39 ± 0.07	1.77						
ΔT (yrs)	East	-0.49 ± 0.06	-0.29 ± 0.06	0.19 ± 0.06	-0.09 ± 0.06	1.65						
3.5948	Up	-4.06 ± 0.19	-1.43 ± 0.19	0.29 ± 0.19	-0.01 ± 0.19	4.71						
BZRG	North	1.44 ± 0.05	0.36 ± 0.06	0.00 ± 0.05	-0.13 ± 0.05	1.58	29/11/2000	3.81 ± 0.16				
ΔT (yrs)	East	-0.06 ± 0.07	-0.37 ± 0.07	0.01 ± 0.06	-0.32 ± 0.06	1.85	29/11/2000	-2.06 ± 0.21				
5.9959	Up	-2.99 ± 0.18	-1.78 ± 0.18	-0.03 ± 0.18	-0.04 ± 0.18	5.17	29/11/2000	-20.12 ± 0.52				
CADM	North	0.26 ± 0.08	0.34 ± 0.08	0.56 ± 0.08	0.05 ± 0.07	1.29						
ΔT (yrs)	East	-1.75 ± 0.11	-1.00 ± 0.12	0.65 ± 0.11	0.33 ± 0.10	1.77						
3.1786	Up	-3.18 ± 0.29	0.73 ± 0.30	1.61 ± 0.28	1.22 ± 0.26	4.56						
CAGL	North	-0.56 ± 0.05	-0.15 ± 0.05	0.06 ± 0.05	-0.02 ± 0.05	1.54	11/07/2001	-1.36 ± 0.13				
ΔT (yrs)	East	-1.89 ± 0.07	-0.64 ± 0.07	0.13 ± 0.07	-0.04 ± 0.07	2.14	11/07/2001	4.22 ± 0.20				
5.8617	Up	-2.72 ± 0.17	2.04 ± 0.17	0.40 ± 0.17	-0.48 ± 0.17	5.28	11/07/2001	0.35 ± 0.46				
CAME	North	-0.35 ± 0.09	0.16 ± 0.09	-0.09 ± 0.08	-0.15 ± 0.08	1.57	15/12/2003	1.27 ± 0.35				
ΔT (yrs)	East	-0.81 ± 0.11	-0.61 ± 0.11	0.23 ± 0.10	-0.07 ± 0.10	2.08	15/12/2003	3.11 ± 0.41				
3.6769	Up	-0.71 ± 0.32	-0.32 ± 0.30	0.99 ± 0.28	-0.54 ± 0.28	6.06	15/12/2003	11.29 ± 1.27				
COSE	North	0.12 ± 0.09	0.22 ± 0.10	0.50 ± 0.09	-0.02 ± 0.10	1.44						
ΔT (yrs)	East	-0.90 ± 0.14	0.18 ± 0.15	0.33 ± 0.14	0.20 ± 0.16	2.22						
3.3484	Up	-1.98 ± 0.37	2.93 ± 0.38	-0.86 ± 0.37	0.33 ± 0.40	5.65						
DUBR	North	-1.05 ± 0.07	-0.77 ± 0.07	-0.48 ± 0.07	0.00 ± 0.07	1.61						
ΔT (yrs)	East	-0.36 ± 0.08	0.88 ± 0.08	0.30 ± 0.08	-0.35 ± 0.08	1.74						
3.2745	Up	-3.97 ± 0.19	-0.55 ± 0.19	0.28 ± 0.18	0.90 ± 0.18	4.1						
ELBA	North	0.21 ± 0.07	0.28 ± 0.07	-0.15 ± 0.07	-0.48 ± 0.07	1.62						
ΔT (yrs)	East	-0.28 ± 0.09	-0.24 ± 0.09	0.02 ± 0.09	-0.27 ± 0.09	2.05						
3.1431	Up	-3.23 ± 0.23	-0.85 ± 0.24	0.88 ± 0.23	-0.84 ± 0.23	5.33	30/03/2003	5.39 ± 0.58				
GENO	North	0.57 ± 0.05	0.54 ± 0.05	0.08 ± 0.05	-0.22 ± 0.05	1.61						
ΔT (yrs)	East	-0.10 ± 9.06	0.17 ± 0.06	0.14 ± 0.06	-0.41 ± 0.06	1.8						
5.4428	Up	-2.35 ± 0.17	-0.21 ± 0.17	-1.19 ± 0.17	-0.03 ± 0.17	5.23						
GRAS	North	0.01 ± 0.04	0.61 ± 0.04	0.25 ± 0.04	-0.33 ± 0.04	1.15	23/04/2003	-0.83 ± 0.12				
ΔT (yrs)	East	-0.33 ± 0.06	0.17 ± 0.05	0.15 ± 0.05	-0.33 ± 0.05	1.59	23/04/2003	2.61 ± 0.14				

5.8261	Up	-1.42 ± 0.13	0.61 ± 0.13	-0.43 ± 0.12	-0.93 ± 0.13	3.6	23/04/2003	3.74 ± 0.37		
GRAZ	North	0.15 ± 0.03	-0.10 ± 0.03	0.17 ± 0.03	0.17 ± 0.03	0.97			07/05/2001	-1.46 ± 0.10
ΔT (yrs)	East	0.08 ± 0.04	0.00 ± 0.04	0.08 ± 0.04	-0.25 ± 0.04	1.31			07/05/2001	-2.30 ± 0.14
5.9959	Up	-3.48 ± 0.13	-0.68 ± 0.12	0.06 ± 0.12	0.10 ± 0.12	3.71	01/07/2000	4.20 ± 0.37	07/05/2001	-0.68 ± 0.38
INGR	North	0.42 ± 0.07	0.78 ± 0.07	-0.23 ± 0.06	-0.16 ± 0.07	1.5				
ΔT (yrs)	East	2.58 ± 0.08	1.20 ± 0.08	0.27 ± 0.08	-0.23 ± 0.08	1.88				
3.5975	Up	-2.91 ± 0.20	-1.02 ± 0.21	0.72 ± 0.19	0.08 ± 0.19	4.48	25/01/2002	-9.66 ± 0.60	28/05/2002	9.29 ± 0.62
LAMP	North	-0.70 ± 0.06	0.030 ± 0.06	-0.12 ± 0.06	-0.22 ± 0.06	1.61				
ΔT (yrs)	East	-1.06 ± 0.07	-0.03 ± 0.07	0.37 ± 0.07	-0.35 ± 0.07	2.07				
4.7666	Up	-2.87 ± 0.18	2.57 ± 0.18	1.13 ± 0.18	0.49 ± 0.18	5.1				
MATE	North	-0.04 ± 0.04	-0.05 ± 0.04	0.07 ± 0.04	-0.11 ± 0.04	1.26	18/06/1999	-3.10 ± 0.12		
ΔT (yrs)	East	0.44 ± 0.05	-0.13 ± 0.05	0.04 ± 0.05	0.08 ± 0.05	1.6	18/06/1999	3.75 ± 0.16		
5.9959	Up	-3.18 ± 0.12	0.10 ± 0.13	0.11 ± 0.12	0.59 ± 0.12	3.98	18/06/1999	3.27 ± 0.39	22/08/2002	-5.59 ± 0.36
MEDI	North	-0.22 ± 0.05	-0.91 ± 0.05	0.29 ± 0.05	0.17 ± 0.05	1.51	03/04/2001	-3.78 ± 0.14		
ΔT (yrs)	East	-0.01 ± 0.07	1.18 ± 0.06	0.13 ± 0.06	-0.49 ± 0.07	1.96	03/04/2001	0.10 ± 0.20		
5.9959	Up	-3.94 ± 0.15	0.01 ± 0.14	-0.35 ± 0.14	0.36 ± 0.14	4.27	03/04/2001	-7.40 ± 0.40		
NOT1	North	0.62 ± 0.07	0.96 ± 0.07	-0.24 ± 0.07	-0.31 ± 0.07	1.62				
ΔT (yrs)	East	-1.44 ± 0.10	-0.22 ± 0.10	-0.17 ± 0.10	-0.09 ± 0.10	2.4				
3.3128	Up	-2.08 ± 0.23	1.16 ± 0.23	0.34 ± 0.23	0.40 ± 0.23	5.38				
NOVA	North	1.65 ± 0.07	0.42 ± 0.08	-0.15 ± 0.07	-0.00 ± 0.07	1.44				
ΔT (yrs)	East	-0.45 ± 0.07	-0.12 ± 0.09	0.19 ± 0.08	-0.05 ± 0.07	1.5				
3.5318	Up	-2.60 ± 0.20	1.12 ± 0.22	-1.26 ± 0.21	-0.20 ± 0.21	4.23				
OBER	North	-0.07 ± 0.04	0.06 ± 0.04	0.49 ± 0.04	0.16 ± 0.04	0.99				
ΔT (yrs)	East	-0.29 ± 0.06	0.07 ± 0.06	0.11 ± 0.06	-0.07 ± 0.06	1.33				
3.4634	Up	-1.97 ± 0.17	-0.09 ± 0.16	-0.39 ± 0.16	0.33 ± 0.16	3.76				
ORID	North	-0.10 ± 0.06	0.08 ± 0.07	-0.14 ± 0.06	-0.10 ± 0.06	1.24				
ΔT (yrs)	East	0.07 ± 0.09	-0.36 ± 0.10	0.30 ± 0.09	-0.17 ± 0.09	1.8				
3.4661	Up	-1.99 ± 0.25	-2.05 ± 0.28	-0.36 ± 0.24	0.86 ± 0.25	4.65				
OSJE	North	-0.75 ± 0.05	0.46 ± 0.05	0.11 ± 0.05	-0.09 ± 0.05	1.17				
ΔT (yrs)	East	-0.56 ± 0.07	-0.28 ± 0.07	0.11 ± 0.07	-0.10 ± 0.07	1.59				
3.2827	Up	-1.74 ± 0.13	-3.41 ± 0.19	-0.04 ± 0.18	0.38 ± 0.18	4.2				
PRAT	North	-0.19 ± 0.07	-0.15 ± 0.07	0.23 ± 0.07	0.20 ± 0.07	1.97				
ΔT (yrs)	East	-0.27 ± 0.06	0.47 ± 0.06	0.20 ± 0.06	-0.14 ± 0.06	1.68				
5.6509	Up	-2.28 ± 0.17	0.10 ± 0.17	-0.59 ± 0.17	0.09 ± 0.17	4.97				
SRJV	North	0.55 ± 0.09	1.04 ± 0.09	0.06 ± 0.08	-0.17 ± 0.08	1.68				
ΔT (yrs)	East	0.06 ± 0.09	0.17 ± 0.11	-0.31 ± 0.09	-0.39 ± 0.09	1.75				
4.46	Up	-2.48 ± 0.25	1.38 ± 0.27	0.24 ± 0.24	0.20 ± 0.24	4.82	14/06/2003	9..95 ± 0.62		

TGRC	North	-0.52 ± 0.09	-0.02 ± 0.09	-0.10 ± 0.09	-0.04 ± 0.09	2.08						
ΔT (yrs)	East	-0.52 ± 0.14	0.30 ± 0.14	0.92 ± 0.14	0.40 ± 0.14	3.28						
3.4497	Up	-2.52 ± 0.31	1.18 ± 0.32	0.83 ± 0.32	2.40 ± 0.31	7.24						
TORI	North	-1.10 ± 0.05	0.17 ± 0.05	-0.02 ± 0.05	0.06 ± 0.05	1.42						
ΔT (yrs)	East	1.01 ± 0.06	0.05 ± 0.06	0.01 ± 0.06	-0.20 ± 0.06	1.74						
5.7851	Up	-3.79 ± 0.18	-1.01 ± 0.18	0.25 ± 0.18	0.25 ± 0.18	5.35						
UNPG	North	-0.44 ± 0.05	-0.19 ± 0.05	0.31 ± 0.05	0.01 ± 0.05	1.36	19/05/2002	-7.33 ± 0.16				
ΔT (yrs)	East	0.38 ± 0.06	0.05 ± 0.06	0.27 ± 0.06	-0.33 ± 0.06	1.74						
5.7851	Up	-2.95 ± 0.17	0.91 ± 0.16	-0.20 ± 0.16	-0.01 ± 0.16	4.63	23/11/1998	-18.48 ± 0.48	10/02/2000	10.33 ± 0.50	25/11/2000	5.15 ± 0.51
UPAD	North	0.99 ± 0.06	-0.02 ± 0.05	0.14 ± 0.06	0.17 ± 0.05	1.32						
ΔT (yrs)	East	-1.32 ± 0.07	-0.77 ± 0.06	0.30 ± 0.07	0.19 ± 0.06	1.54						
3.8741	Up	-3.49 ± 0.19	1.35 ± 0.18	-0.72 ± 0.18	0.14 ± 0.18	4.31						
VENE	North	2.40 ± 0.06	0.84 ± 0.07	0.59 ± 0.06	-0.96 ± 0.06	1.83			01/02/2001	3.20 ± 0.17		
ΔT (yrs)	East	-1.78 ± 0.06	-1.38 ± 0.06	0.13 ± 0.06	0.56 ± 0.06	1.68			01/02/2001	1.13 ± 0.17		
5.9959	Up	-4.00 ± 0.20	0.22 ± 0.23	-0.08 ± 0.20	0.29 ± 0.20	5.84	22/08/1999	-52.99 ± 0.68	01/02/2001	94.53 ± 0.64	15/12/2001	10..34 ± 0.54
VLUC	North	-0.66 ± 0.08	0.28 ± 0.08	0.15 ± 0.08	-0.03 ± 0.08	1.71						
ΔT (yrs)	East	-0.24 ± 0.10	-0.47 ± 0.10	0.35 ± 0.10	-0.00 ± 0.10	2.16						
5.4073	Up	-4.83 ± 0.24	-0.79 ± 0.24	0.91 ± 0.24	1.22 ± 0.23	5.14						
VVLO	North	-0.65 ± 0.08	0.49 ± 0.09	-0.00 ± 0.09	0.06 ± 0.09	1.92	31/08/2001	-2.36 ± 0.27	11/01/2003	1.09 ± 0.26		
ΔT (yrs)	East	0.28 ± 0.09	0.03 ± 0.10	-0.29 ± 0.10	-0.09 ± 0.09	2.11						
3.5838	Up	-2.76 ± 0.26	-0.14 ± 0.27	1.38 ± 0.27	1.64 ± 0.26	5.9	31/08/2001	-2.00 ± 0.82	11/01/2003	5.70 ± 0.79		
ZIMM	North	-0.10 ± 0.03	-0.15 ± 0.03	0.09 ± 0.03	0.02 ± 0.03	1.06	06/11/1998	0.98 ± 0.10				
ΔT (yrs)	East	-0.31 ± 0.04	-0.03 ± 0.05	-0.02 ± 0.04	-0.31 ± 0.04	1.41	06/11/1998	3.01 ± 0.13				
5.9959	Up	-1.62 ± 0.12	-0.58 ± 0.12	-0.58 ± 0.12	-0.39 ± 0.12	3.78	06/11/1998	-11.63 ± 0.34				

Tab. 3

Site	Velocity (mm/yr)		Uncertainty (mm/yr)		Residual velocity (mm/yr)		Velocità (mm(yr)	Uncertainty (mm(yr)	Residual Velocity (mm/yr)
ID	East	North	East	North	East	North	Vertical	Vertical	Vertical
AJAC	21.11	14.69	0.55	0.58	-0.12	-0.40	-0.60	1.32	0.60
AQUI	20.72	15.69	0.48	0.49	-1.23	1.18	0.56	1.01	1.76
BRAS	21.81	16.08	0.54	0.57	0.56	1.28	1.08	1.26	2.28
BZRG	19.67	14.61	0.41	0.42	-1.18	-0.16	0.82	0.79	2.02
CADM	23.66	18.17	0.57	0.59	1.03	4.08	0.75	1.45	1.95
CAGL	21.85	15.28	0.42	0.44	0.12	0.21	-1.80	0.82	-0.60
CAME	22.42	17.19	0.59	0.61	0.63	2.65	-2.91	1.49	-1.71
COSE	23.66	16.65	0.55	0.57	0.76	2.57	-3.20	1.40	-2.00
DUBR	22.40	16.84	0.56	0.58	-0.30	3.04	-1.16	1.35	0.04
ELBA	20.76	15.10	0.57	0.60	-0.58	0.19	-0.60	1.40	0.60
GENO	21.11	14.87	0.43	0.44	0.31	-0.20	-1.09	0.85	0.11
GRAS	20.86	15.38	0.42	0.43	0.30	0.09	-2.02	0.82	-0.82
GRAZ	22.29	14.64	0.41	0.42	0.79	0.44	-1.52	0.80	-0.32
INGR	22.02	16.21	0.53	0.55	0.13	1.59	-0.79	1.24	0.41
LAMP	20.33	17.74	0.46	0.48	-2.47	3.13	-0.15	0.96	1.05
MATE	23.85	18.46	0.41	0.43	1.09	4.44	1.08	0.80	2.28
MEDI	22.81	17.50	0.41	0.42	1.53	2.77	-2.69	0.79	-1.49
NOT1	21.69	18.75	0.56	0.59	-1.30	4.47	-0.95	1.35	0.25
NOVA	20.14	14.89	0.53	0.55	-0.41	-0.21	-0.09	1.28	1.11
ORID	24.46	9.72	0.58	0.60	1.13	-3.65	-1.94	1.46	-0.74
OSJE	22.01	14.05	0.56	0.58	-0.32	0.34	-2.34	1.36	-1.14
PRAT	22.16	17.12	0.42	0.44	0.87	2.32	-2.09	0.83	-0.89
SRJV	22.95	15.16	0.56	0.58	0.39	1.41	0.75	1.38	1.95
TGRC	24.12	16.27	0.55	0.57	1.18	2.09	-0.23	1.31	0.97
TORI	20.87	15.01	0.42	0.43	0.43	-0.20	-0.72	0.82	0.48
UNPG	21.93	15.94	0.42	0.43	0.28	1.30	0.40	0.82	1.60
UPAD	21.61	16.87	0.51	0.53	0.46	2.17	-3.61	1.17	-2.41
VENE	22.22	15.47	0.41	0.42	0.99	0.83	-0.24	0.80	0.96
VLUC	22.27	16.39	0.43	0.45	-0.32	2.15	-0.14	0.91	1.06
VVLO	22.81	18.10	0.53	0.57	0.74	3.63	0.95	1.26	2.15
ZIMM	20.26	15.21	0.41	0.42	0.23	-0.02	0.16	0.79	1.36

Tab. 4

Source	Range of effects
Pole tide	~4mm
Ocean tide	~0.1mm
Atmospheric mass	~4mm
Non-tidal ocean mass	2-3mm
Snow mass	3-5mm
Soil moisture	2-7mm
Bedrock thermal expansion	~0.5mm
Errors in orbit, phase center, and tropospere models	No quantitative results yet
Error in network adjustment	~0.7mm
Differences from different software	~2-3mm, at some sites 5-7mm

Tab. 5

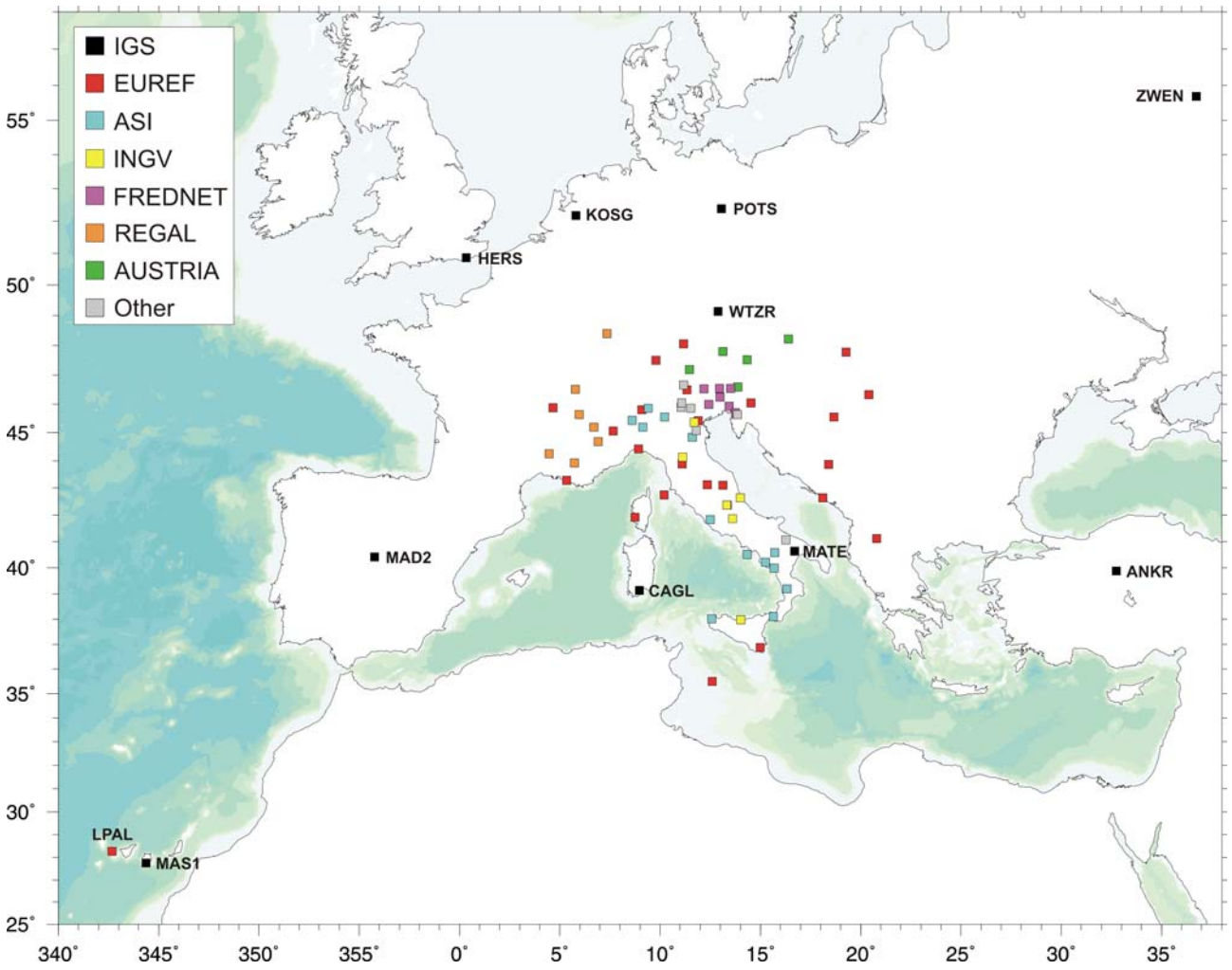
IGS
EUREF
ASI
INGV
FREDNET
REGAL
AUSTRIA
Other
ZWEN
KOSG
POTS
HERS
WTZR
MAD2
MATE
ANKR
CAGL
LPAL
MAS1
55˚
50˚
45˚
40˚
35˚
30˚
25˚
340˚
345˚
350˚
355˚
0˚
5˚
10˚
15˚
20˚
25˚
30˚
35˚

Figure 1a

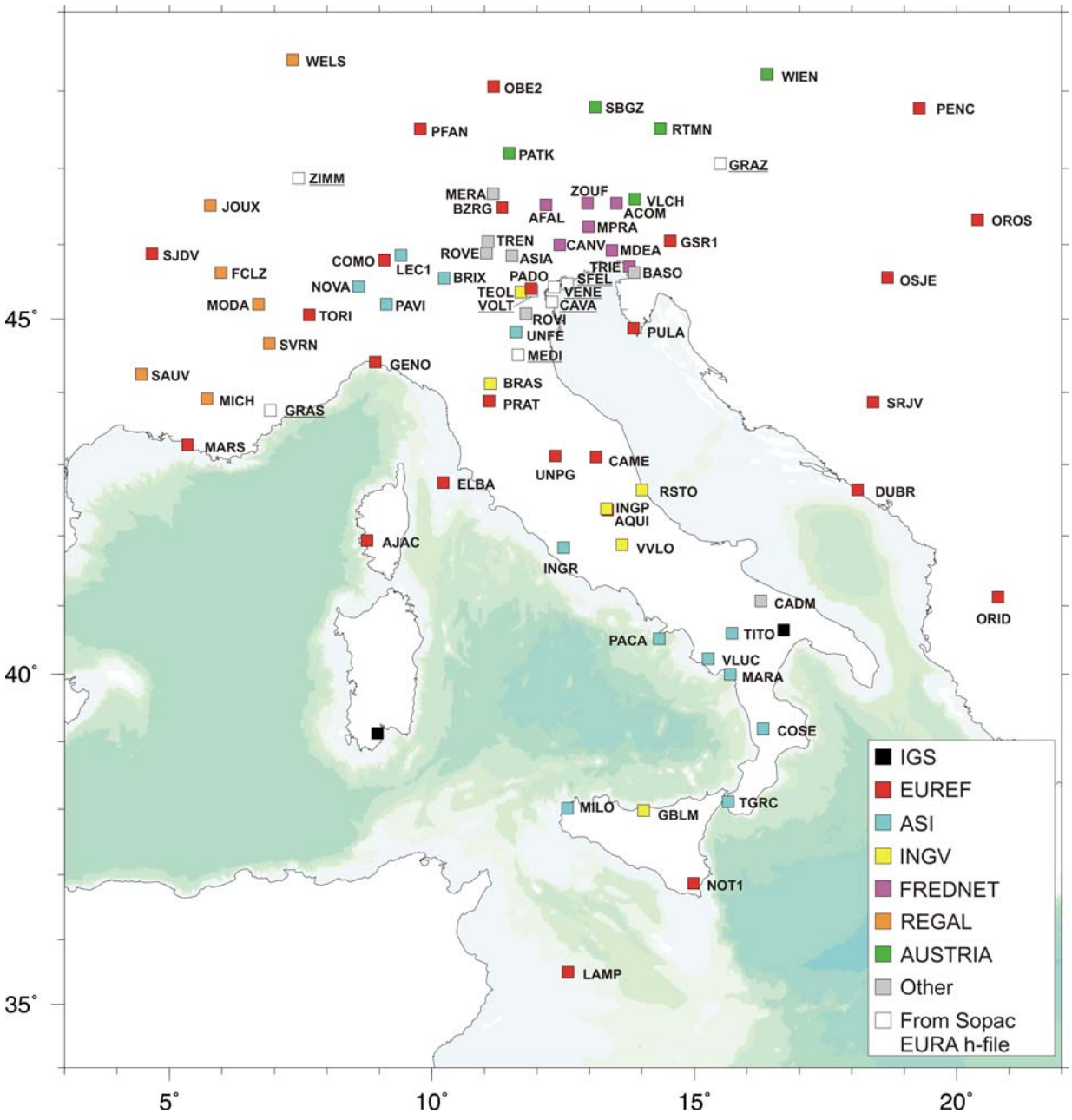
WELS
OBE2
WIEN
SBGZ
PENC
PFAN
RTMN
PATK
GRAZ
ZIMM
JOUX
MERA
BZRG
AFAL
ZOUF
VLCH
ACOM
MPRA
OROS
SJDV
FCLZ
COMO
LEC1
ROVE
TREN
ASIA
CANV
MDEA
GSR1
TRIE
BASO
OSJE
NOVA
BRIX
PADO
SFEL
TEOL
VENE
VOLT
CAVA
MODA
TORI
PAVI
ROVI
PULA
SVRN
UNFE
MEDI
SAUV
GENO
BRAS
MICH
GRAS
PRAT
SRJV
MARS
UNPG
CAME
ELBA
RSTO
DUBR
INGP
AQUI
AJAC
VVLO
INGR
CADM
ORID
TITO
PACA
VLUC
MARA
COSE
MILO
GBLM
TGRC
NOT1
LAMP
IGS
EUREF
ASI
INGV
FREDNET
REGAL
AUSTRIA
Other
From Sopac
EURA h-file
45°
40°
35°
5°
10°
15°
20°

Figure 1b

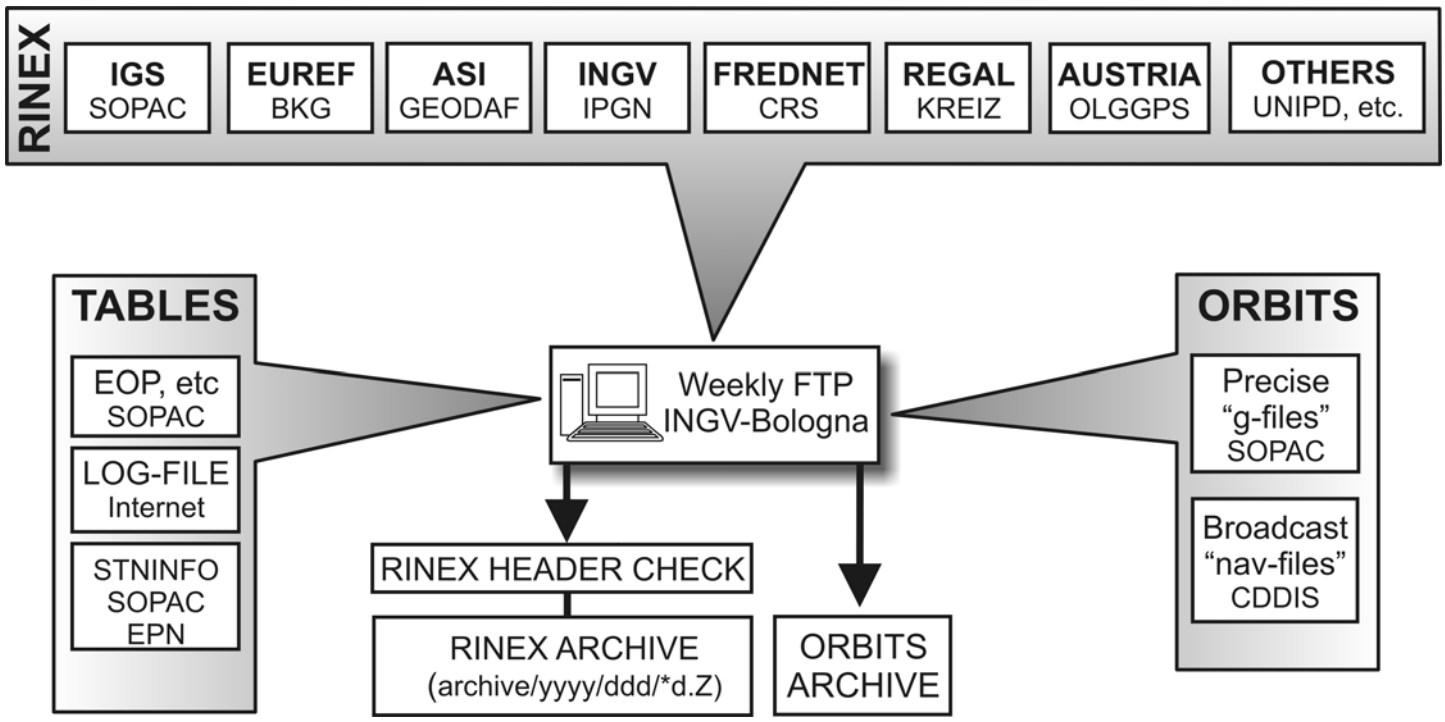
RINEX
IGS
SOPAC
EUREF
BKG
ASI
GEODAF
INGV
IPGN
FREDNET
CRS
REGAL
KREIZ
AUSTRIA
OLGGPS
OTHERS
UNIPD, etc.
TABLES
EOP, etc
SOPAC
LOG-FILE
Internet
STNINFO
SOPAC
EPN
Weekly FTP
INGV-Bologna
ORBITS
Precise
“g-files”
SOPAC
Broadcast
“nav-files”
CDDIS
RINEX HEADER CHECK
RINEX ARCHIVE
(archive/yyyy/ddd/*d.Z)
ORBITS
ARCHIVE

Figure 2

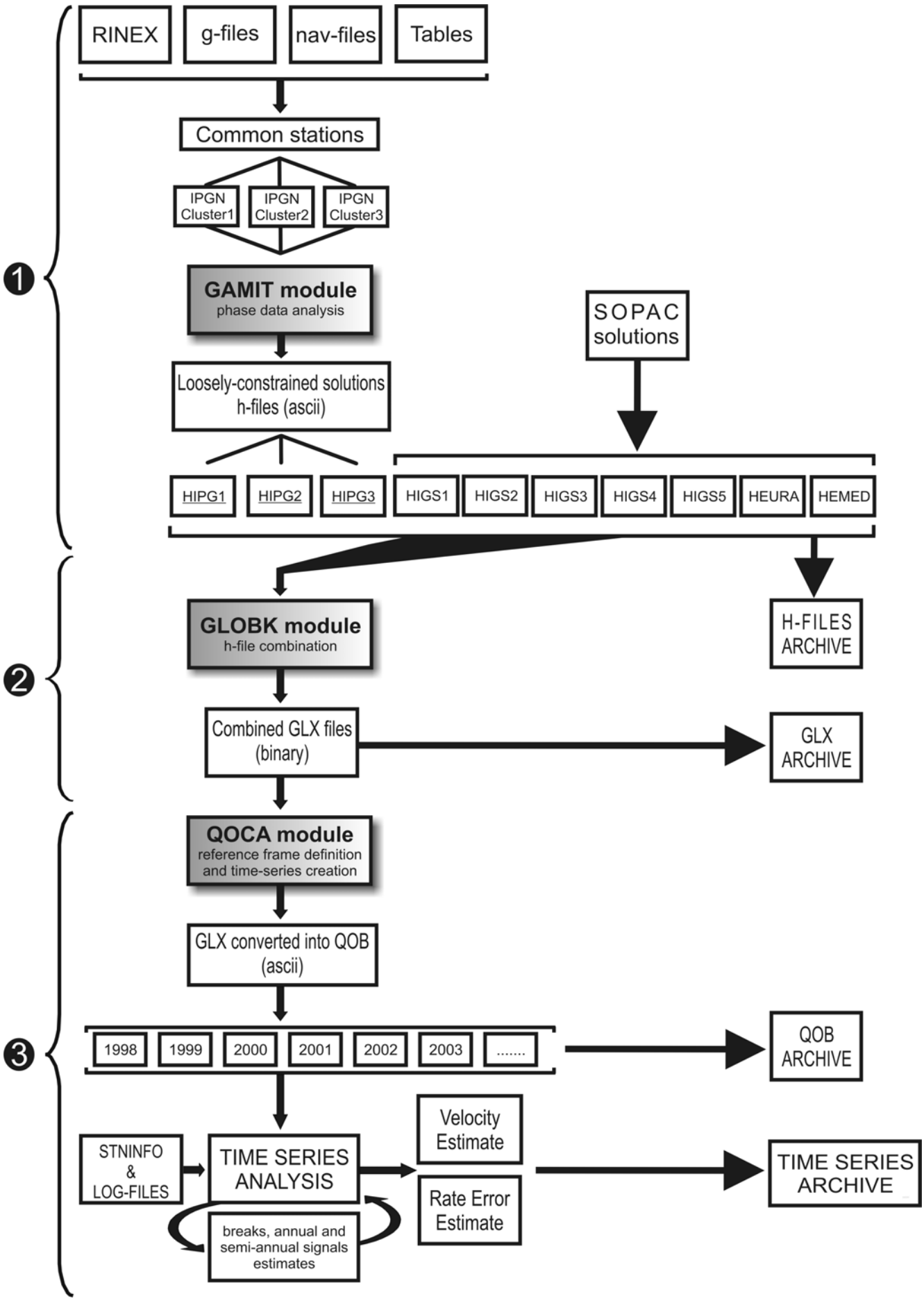
RINEX
g-files
nav-files
Tables
Common stations
IPGN Cluster1
IPGN Cluster2
IPGN Cluster3
GAMIT module
phase data analysis
SOPAC solutions
Loosely-constrained solutions h-files (ascii)
HIPG1
HIPG2
HIPG3
HIGS1
HIGS2
HIGS3
HIGS4
HIGS5
HEURA
HEMED
GLOBK module
h-file combination
H-FILES ARCHIVE
Combined GLX files (binary)
GLX ARCHIVE
QOCA module
reference frame definition and time-series creation
GLX converted into QOB (ascii)
1998
1999
2000
2001
2002
2003
.....
QOB ARCHIVE
STNINFO & LOG-FILES
TIME SERIES ANALYSIS
Velocity Estimate
Rate Error Estimate
TIME SERIES ARCHIVE
breaks, annual and semi-annual signals estimates
1
2
3

Figure 3

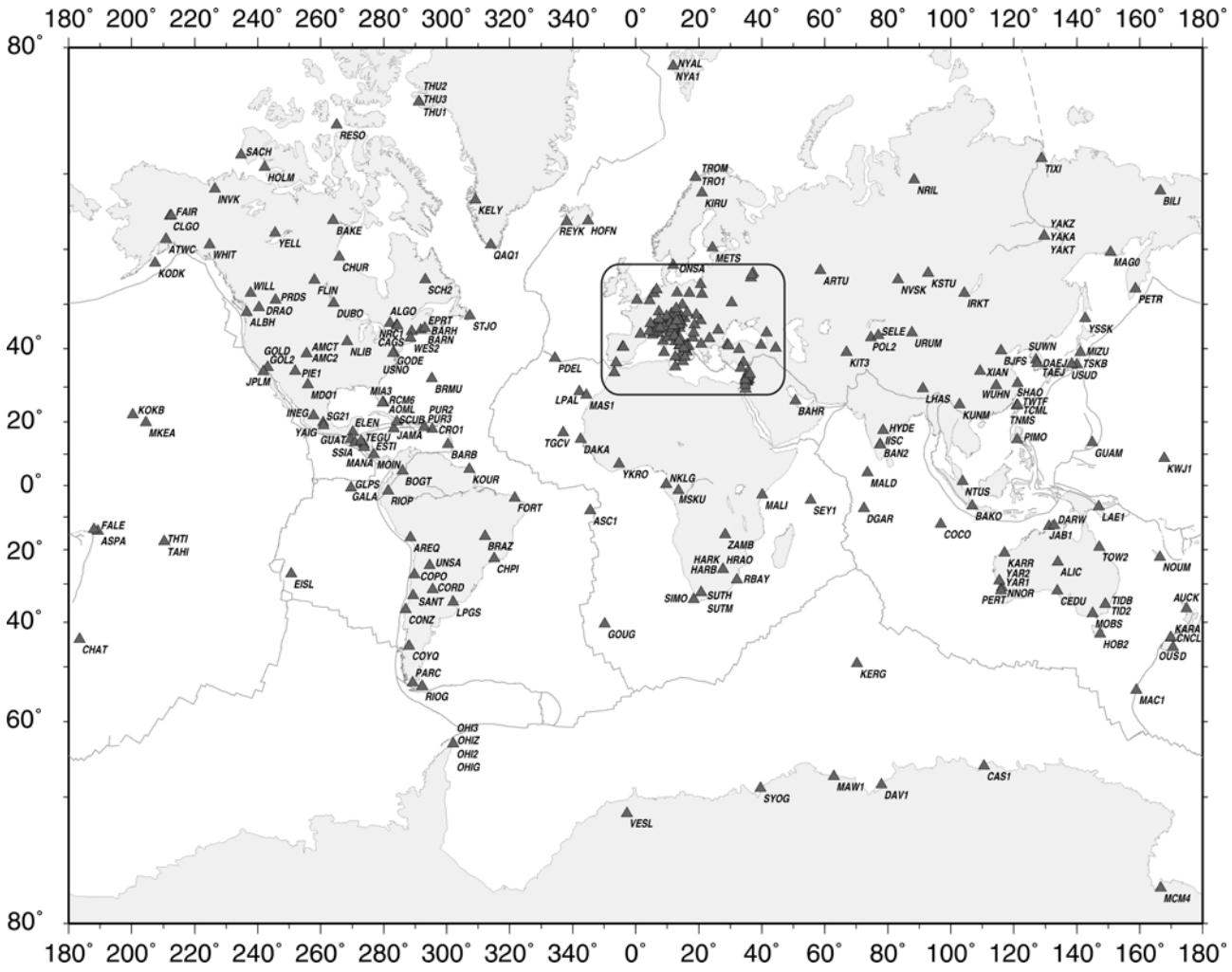
180° 200° 220° 240° 260° 280° 300° 320° 340° 0° 20° 40° 60° 80° 100° 120° 140° 160° 180°
80°
40°
20°
0°
20°
40°
60°
80°
NYAL
NYA1
THU2
THU3
THU1
RESO
SACH
HOLM
INVK
FAIR
CLGO
ATWC
WHIT
KODK
YELL
BAKE
CHUR
KELY
QAQ1
REYK
HOFN
TROM
TRO1
KIRU
METS
ONSA
TIXI
NRIL
BILI
YAKZ
YAKA
YAKT
MAGO
PETR
ARTU
NVSK
KSTU
IRKT
WILL
PRDS
DRAO
ALBH
FLIN
DUBO
SCH2
ALGO
EPRT
BARH
BARN
WES2
STJO
NRC1
CAGS
GOLD
GOL2
AMCT
AMC2
NLIB
GODE
USNO
PIE1
JPLM
PDEL
SELE
POL2
URUM
KIT3
SUWN
MIZU
BJFS
DAEJ
TSKB
TAEJ
USUD
XIAN
WUHN
SHAO
TWTF
TCML
TNMS
LHAS
KUNM
PIMO
BAHR
MDO1
MIA3
BRMU
LPAL
MAS1
KOKB
MKEA
INEG
SG21
YAIG
GUAT
ELEN
SCUB
ACM6
AOML
PUR2
PUR3
CRO1
JAMA
TEGU
ESTI
SSIA
MANA
MOIN
BARB
KOUR
TGCV
DAKA
HYDE
IISC
BAN2
GUAM
KWJ1
YKRO
NKLG
MSKU
MALD
NTUS
GLPS
GALA
BOGT
RIOP
FORT
MALI
SEY1
DGAR
BAKO
COCO
DARW
JAB1
LAE1
ASC1
FALE
ASPA
THTI
TAHI
AREQ
UNSA
COPO
CORD
SANT
CONZ
LPGS
BRAZ
CHPI
EISL
ZAMB
HARK
HRAO
HARB
RBAY
SIMO
SUTH
SUTM
KARR
YAR2
YAR1
PERT
NNOR
ALIC
TOW2
NOUM
CEDU
TIDB
TID2
MOBS
HOB2
AUCK
KARA
CNCL
OUSD
CHAT
GOUG
KERG
MAC1
COYQ
PARC
RIOG
OHI3
OHIZ
OHI2
OHIG
SYOG
MAW1
DAV1
CAS1
VESL
MCM4

Figure 4a

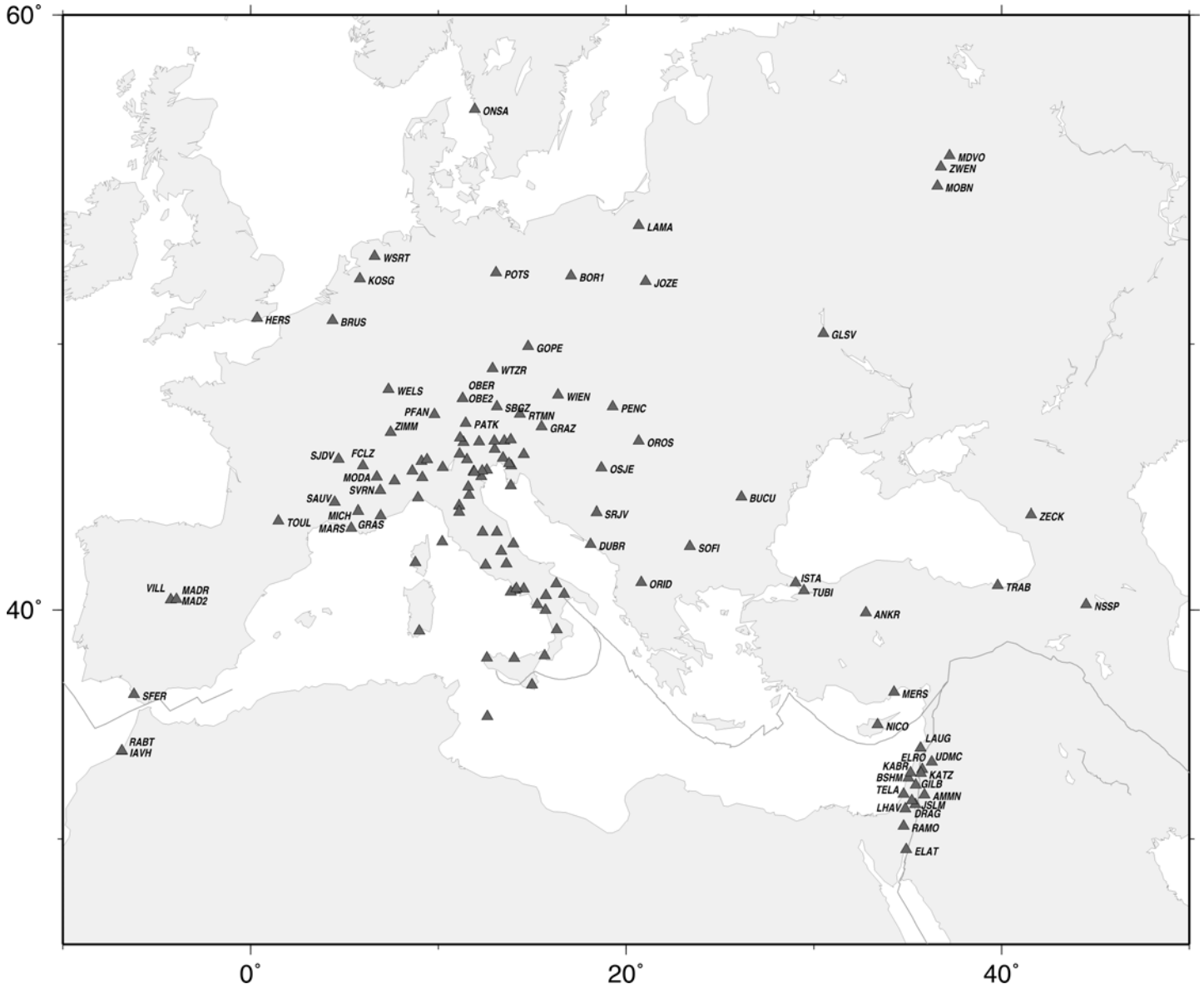
60°
40°
0°
20°
40°
ONSA
MDVO
ZWEN
MOBN
LAMA
WSRT
KOSG
POTS
BOR1
JOZE
HERS
BRUS
GLSV
GOPE
WTZR
WELS
OBER
OBE2
WIEN
PENC
SBGZ
RTMN
PFAN
PATK
ZIMM
GRAZ
OROS
SJDV
FCLZ
OSJE
MODA
SVRN
BUCU
SAUV
SRJV
ZECK
TOUL
MICH
MARS
GRAS
DUBR
SOFI
VILL
MADR
MAD2
ORID
ISTA
TUBI
TRAB
NSSP
ANKR
SFER
MERS
NICO
RABT
IAVH
LAUG
ELRO
UDMC
KABR
KATZ
BSHM
GILB
TELA
AMMN
LHAV
ISLM
DRAG
RAMO
ELAT

Figure 4b

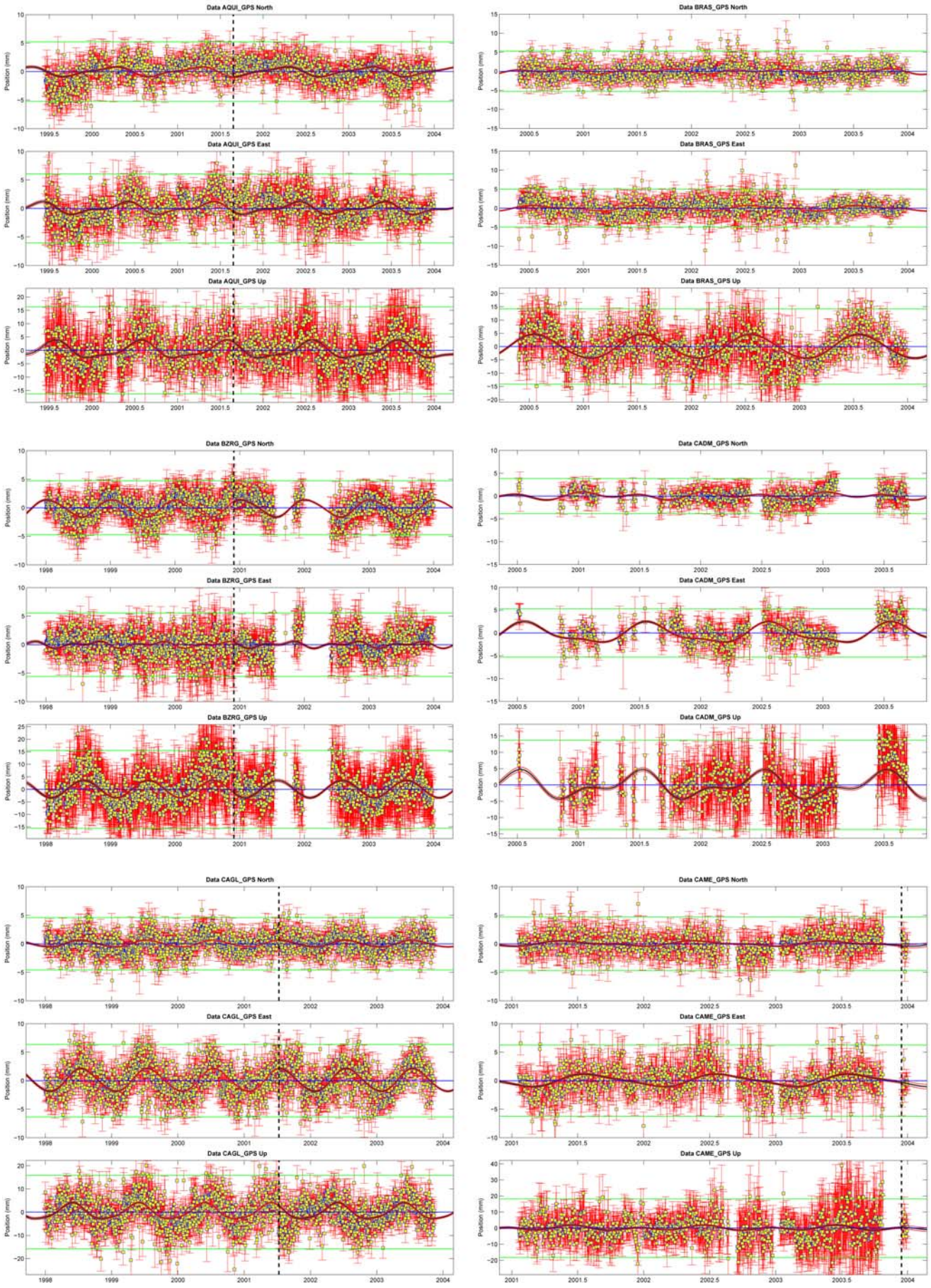
Data AQUI_GPS North
Data AQUI_GPS East
Data AQUI_GPS Up
Data BRAS_GPS North
Data BRAS_GPS East
Data BRAS_GPS Up
Data BZRG_GPS North
Data BZRG_GPS East
Data BZRG_GPS Up
Data CADM_GPS North
Data CADM_GPS East
Data CADM_GPS Up
Data CAGL_GPS North
Data CAGL_GPS East
Data CAGL_GPS Up
Data CAME_GPS North
Data CAME_GPS East
Data CAME_GPS Up
Position (mm)

Figure 5°

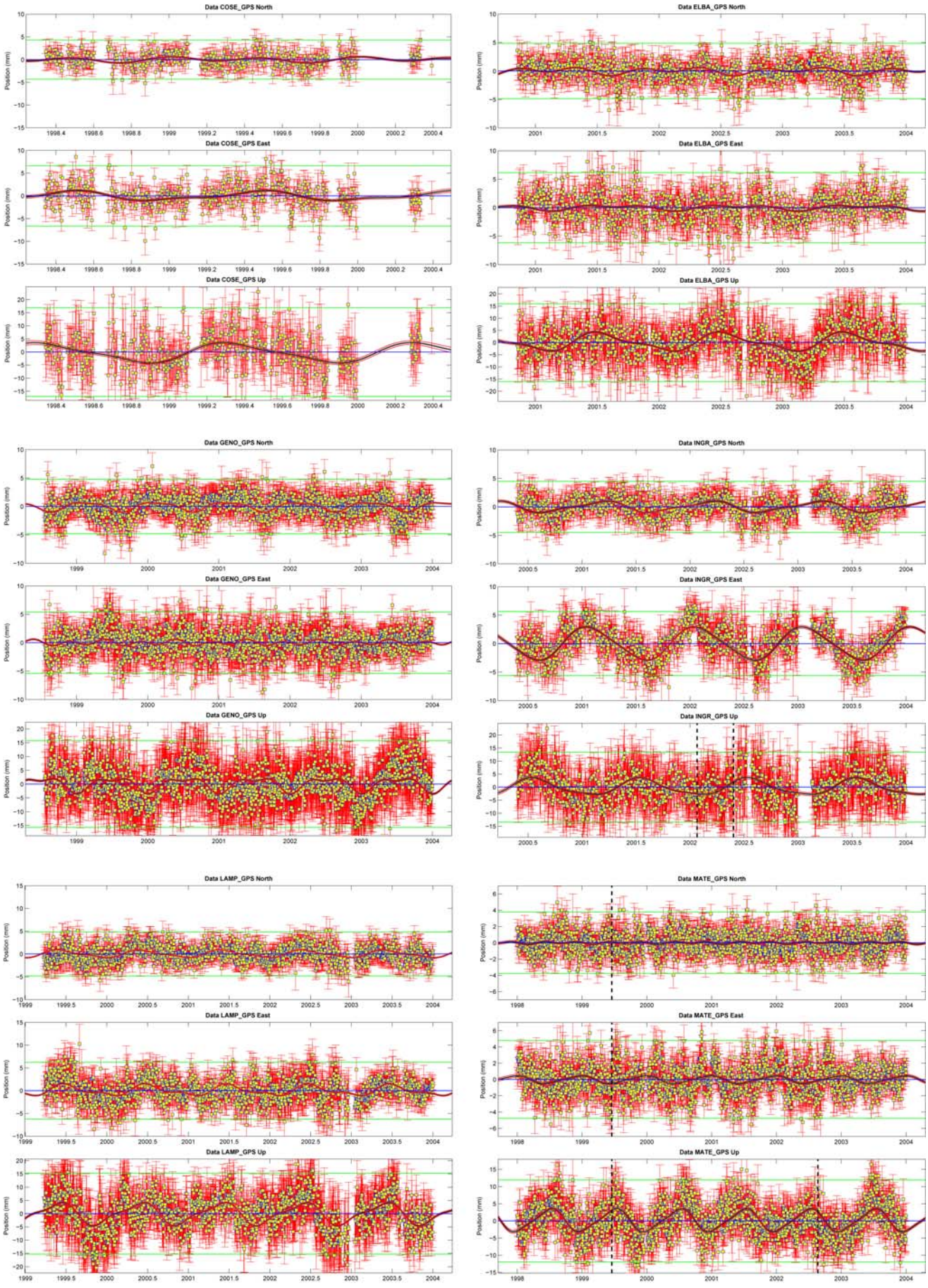
Data COSE_GPS North
Data COSE_GPS East
Data COSE_GPS Up
Data ELBA_GPS North
Data ELBA_GPS East
Data ELBA_GPS Up
Data GENO_GPS North
Data GENO_GPS East
Data GENO_GPS Up
Data INGR_GPS North
Data INGR_GPS East
Data INGR_GPS Up
Data LAMP_GPS North
Data LAMP_GPS East
Data LAMP_GPS Up
Data MATE_GPS North
Data MATE_GPS East
Data MATE_GPS Up
Position (mm)

Figure 5b

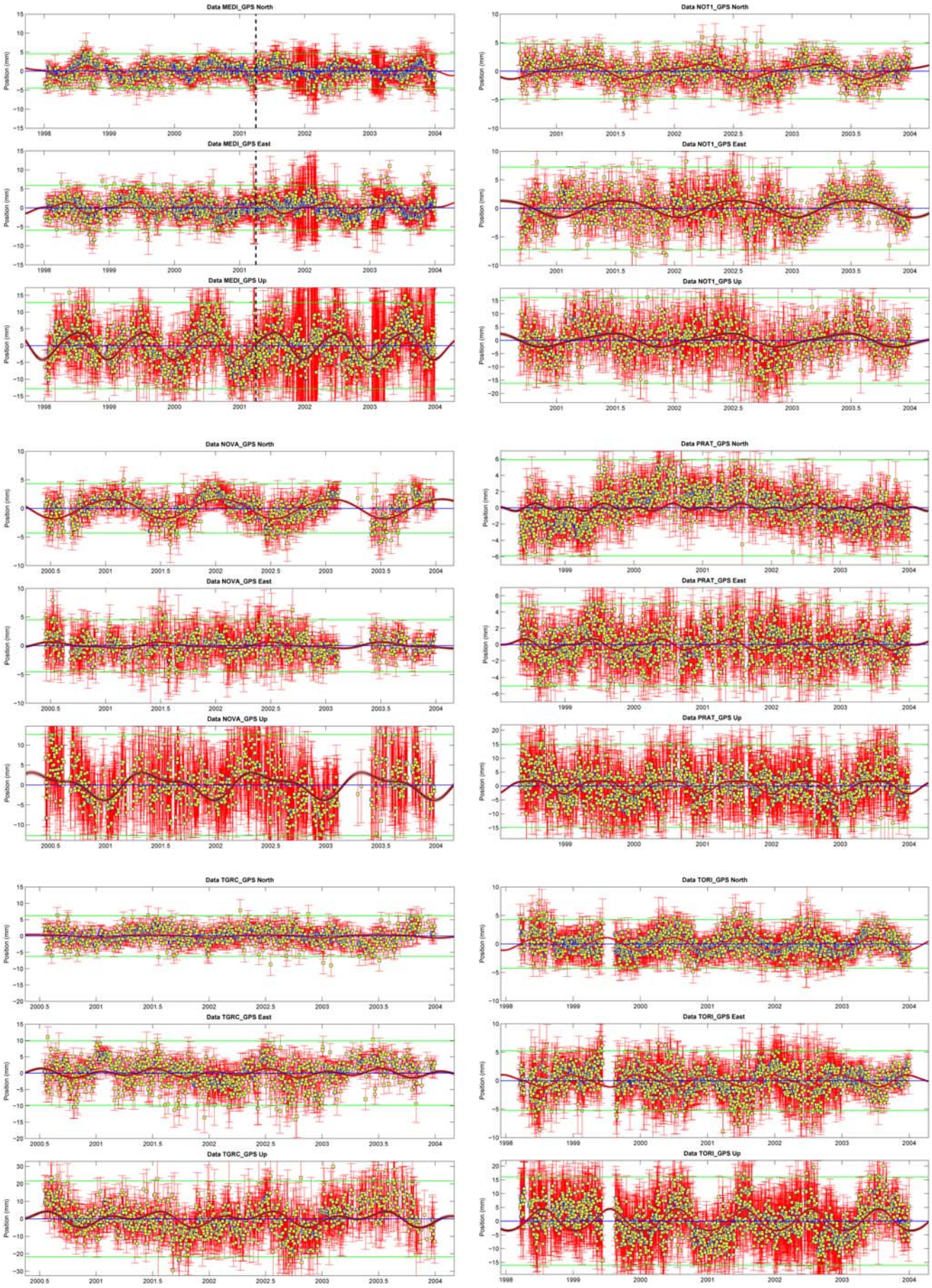
Data MEDI_GPS North
Data MEDI_GPS East
Data MEDI_GPS Up
Data NOT1_GPS North
Data NOT1_GPS East
Data NOT1_GPS Up
Data NOVA_GPS North
Data NOVA_GPS East
Data NOVA_GPS Up
Data PRAT_GPS North
Data PRAT_GPS East
Data PRAT_GPS Up
Data TGRC_GPS North
Data TGRC_GPS East
Data TGRC_GPS Up
Data TORI_GPS North
Data TORI_GPS East
Data TORI_GPS Up
Position (mm)

Figure 5c

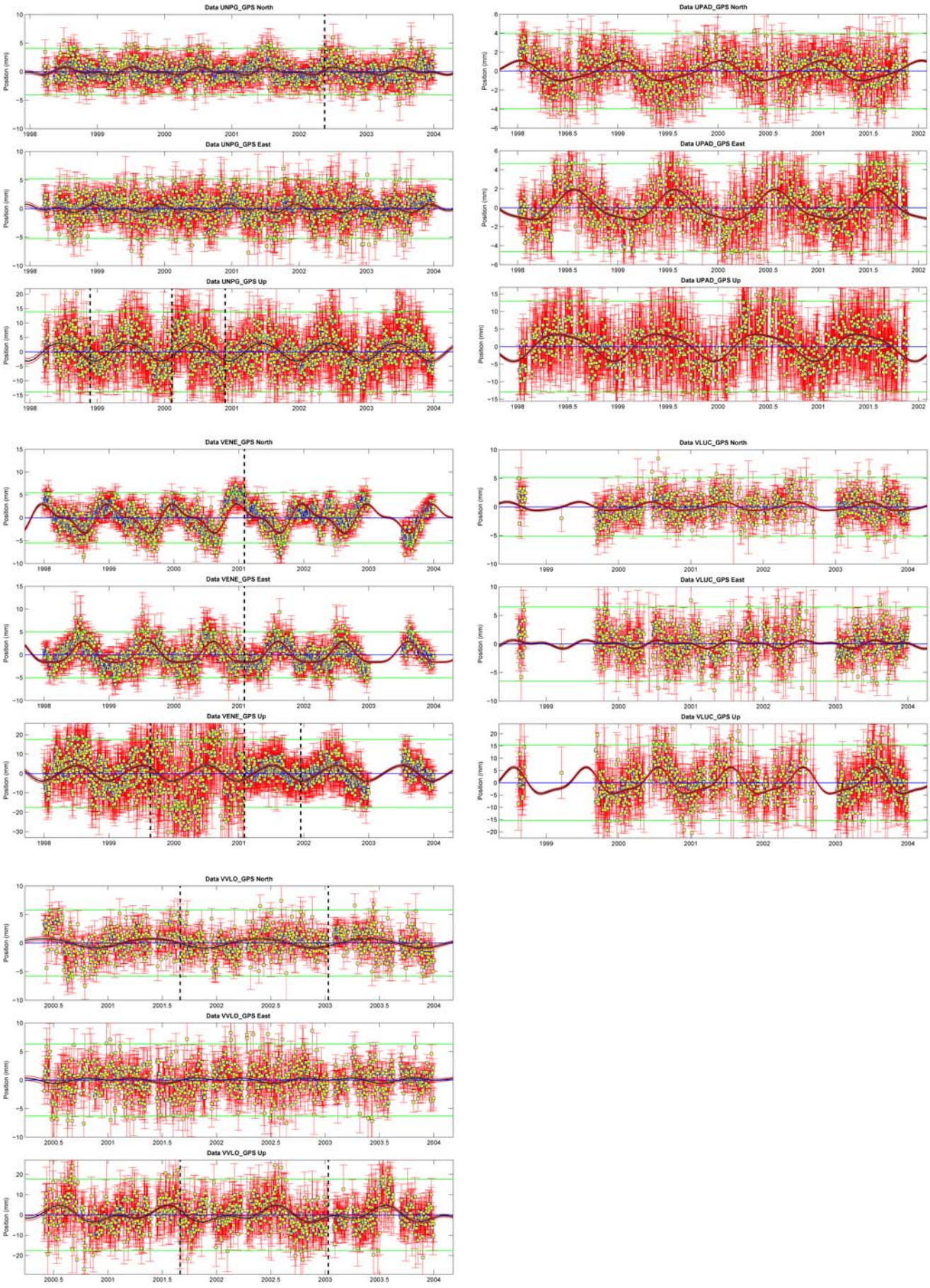
Data UNPG_GPS North
Data UNPG_GPS East
Data UNPG_GPS Up
Data UPAD_GPS North
Data UPAD_GPS East
Data UPAD_GPS Up
Data VENE_GPS North
Data VENE_GPS East
Data VENE_GPS Up
Data VLUC_GPS North
Data VLUC_GPS East
Data VLUC_GPS Up
Data VVLO_GPS North
Data VVLO_GPS East
Data VVLO_GPS Up
Position (mm)

Figure 5d

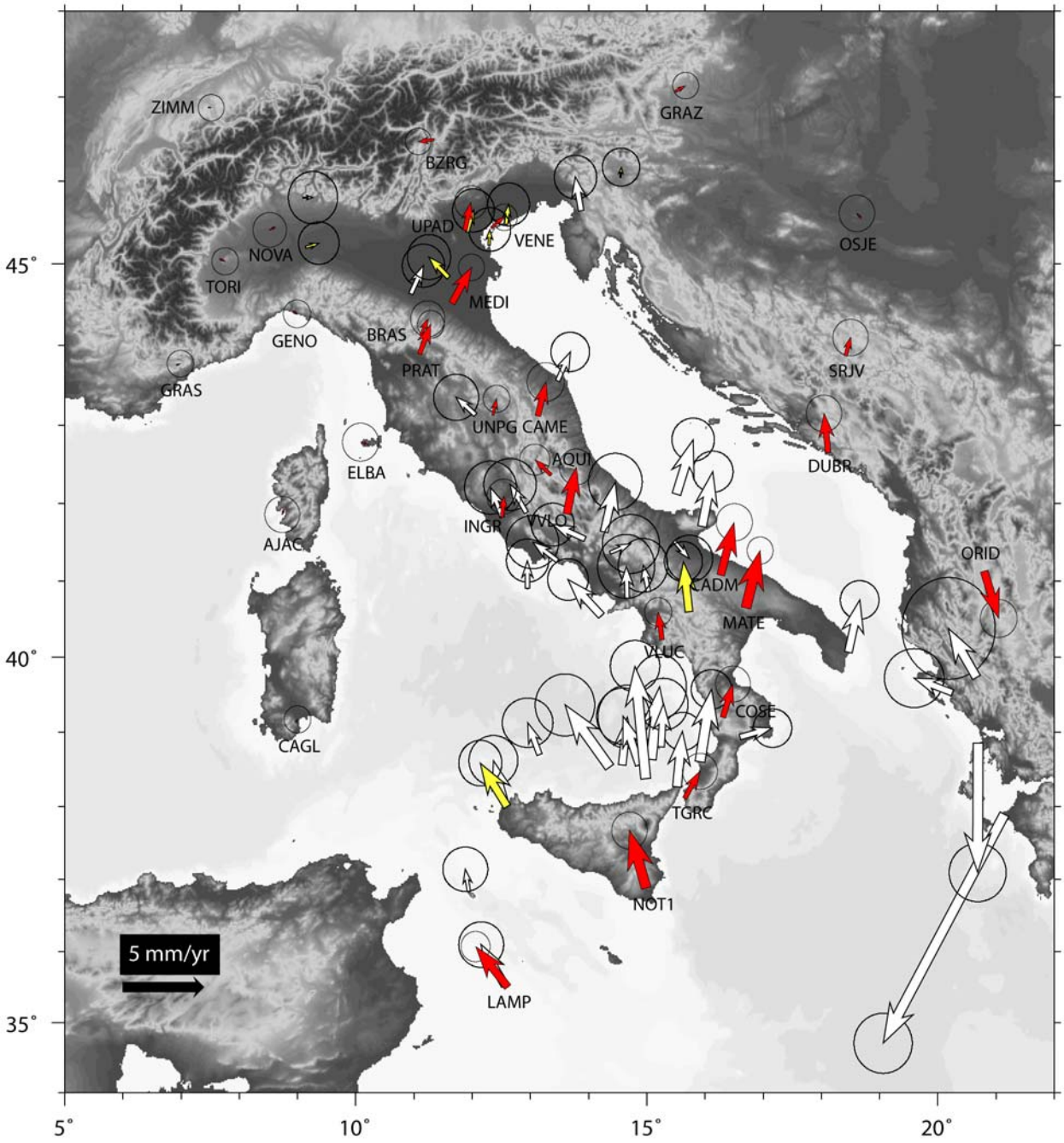
ZIMM
GRAZ
BZRG
UPAD
VENE
OSJE
NOVA
TORI
MEDI
GENO
BRAS
PRAT
GRAS
SRJV
UNPG
CAME
ELBA
AQUI
DUBR
AJAC
INGR
VVLO
ORID
CADM
MATE
VLUC
COSE
CAGL
TGRC
NOT1
5 mm/yr
LAMP
45°
40°
35°
5°
10°
15°
20°

Figure 6a

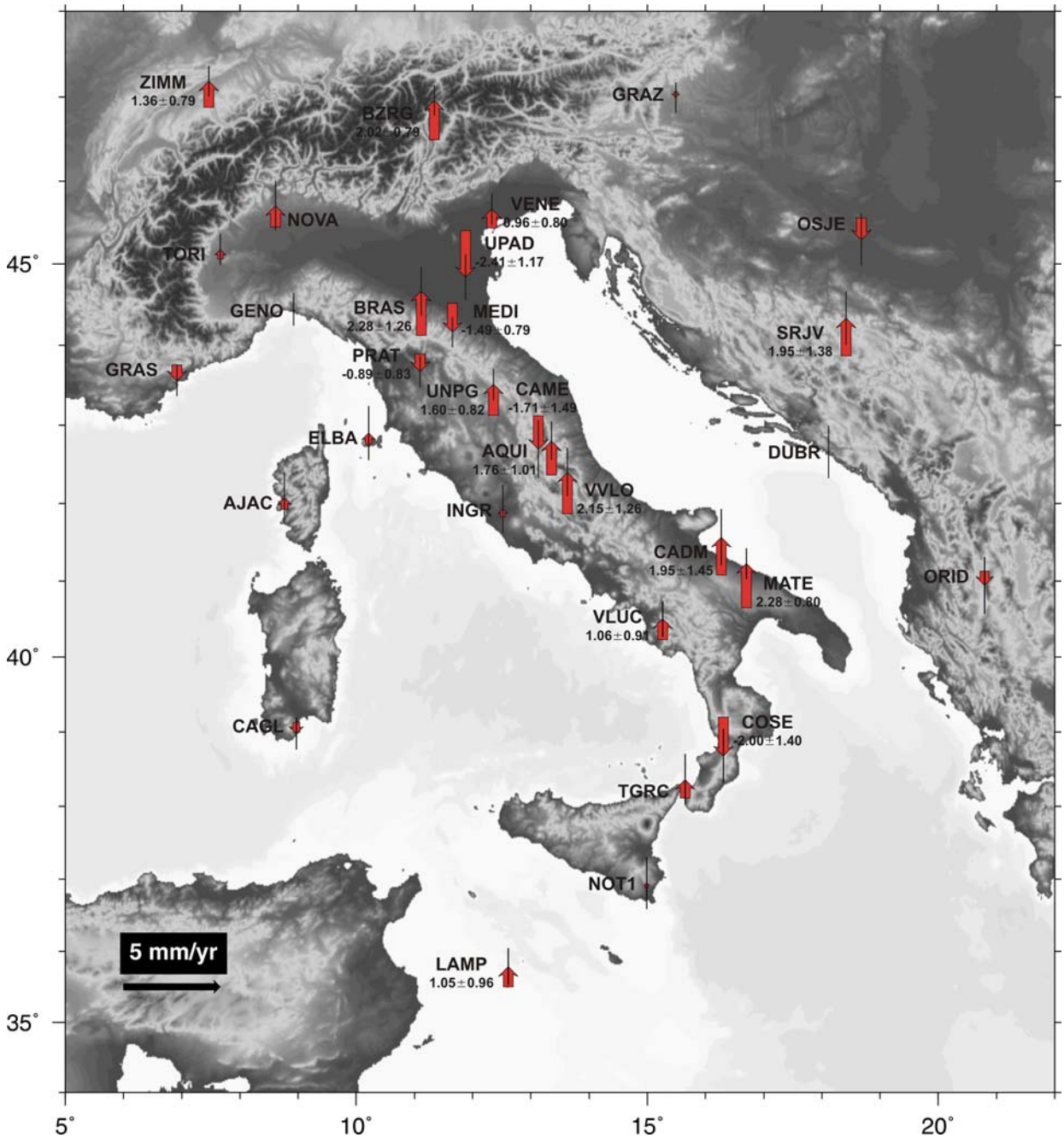
ZIMM
1.36±0.79
BZRG
2.02±0.79
GRAZ
NOVA
VENE
0.96±0.80
OSJE
UPAD
-2.41±1.17
TORI
GENO
BRAS
2.28±1.26
MEDI
-1.49±0.79
SRJV
1.95±1.38
PRAT
-0.89±0.83
GRAS
UNPG
1.60±0.82
CAME
-1.71±1.49
ELBA
AQUI
1.76±1.01
DUBR
VVLO
2.15±1.26
AJAC
INGR
CADM
1.95±1.45
ORID
MATE
2.28±0.80
VLUC
1.06±0.91
CAGL
COSE
2.00±1.40
TGRC
NOT1
5 mm/yr
LAMP
1.05±0.96
45°
40°
35°
5°
10°
15°
20°

Figure 6b